Soft Matter

PAPER

View Article Online
View Journal | View Issue

Cite this: *Soft Matter*, 2017, 13, 8309

Molecular rigidity and enthalpy–entropy compensation in DNA melting

Fernando Vargas-Lara, *[a] Francis W. Starr[b] and Jack F. Douglas*[a]

Received 20th June 2017,
Accepted 24th September 2017

DOI: 10.1039/c7sm01220a

rsc.li/soft-matter-journal

Enthalpy–entropy compensation (EEC) is observed in diverse molecular binding processes of importance to living systems and manufacturing applications, but this widely occurring phenomenon is not sufficiently understood from a molecular physics standpoint. To gain insight into this fundamental problem, we focus on the melting of double-stranded DNA (dsDNA) since measurements exhibiting EEC are extensive for nucleic acid complexes and existing coarse-grained models of DNA allow us to explore the influence of changes in molecular parameters on the energetic parameters by using molecular dynamics simulations. Previous experimental and computational studies have indicated a correlation between EEC and changes in molecular rigidity in certain binding–unbinding processes, and, correspondingly, we estimate measures of DNA molecular rigidity under a wide range of conditions, along with resultant changes in the enthalpy and entropy of binding. In particular, we consider variations in dsDNA rigidity that arise from changes of intrinsic molecular rigidity such as varying the associative interaction strength between the DNA bases, the length of the DNA chains, and the bending stiffness of the individual DNA chains. We also consider extrinsic changes of molecular rigidity arising from the addition of polymer additives and geometrical confinement of DNA between parallel plates. All our computations confirm EEC and indicate that this phenomenon is indeed highly correlated with changes in molecular rigidity. However, two distinct patterns relating to how DNA rigidity influences the entropy of association emerge from our analysis. Increasing the intrinsic DNA rigidity increases the entropy of binding, but increases in molecular rigidity from external constraints decreases the entropy of binding. EEC arises in numerous synthetic and biological binding processes and we suggest that changes in molecular rigidity might provide a common origin of this ubiquitous phenomenon in the mutual binding and unbinding of complex molecules.

I. Introduction

Molecular binding and unbinding[1,2] is central to the organization and function of biological systems and includes such basic processes as the expression of genetic information,[3,4] RNA switches regulating cell activities,[5–7] molecular recognition,[8–10] protein folding and unfolding,[11] the self-assembly of actin[12] and other proteins of the cytoplasm and the extracellular matrix, and the formation of double stranded DNA (dsDNA),[13,14] *etc.* Molecular and nanoparticle association are also central to the formation and stability of synthetic structures formed by self-assembly in manufacturing applications, *e.g.*, the formation of lattices of nanoparticles connected by dsDNA,[15,16] DNA origami tiles organized into nanotubes,[17] the separation of carbon nanotubes by chirality by wrapping these nanoparticles with DNA,[18] which are just a few representative materials science examples. In living systems, binding processes must be tightly regulated, and many diseases result from a breakdown of regulation processes of binding phenomena that disrupt biological functions. Regulating binding processes is likewise crucial in manufacturing applications based on self-assembly.

The study of molecular association of biological and synthetic macromolecules is often greatly complicated by the many internal degrees of freedom within these molecules that become altered in the course of the binding process or by the presence of surrounding molecules that indirectly contribute to the binding thermodynamics. Molecular binding in macromolecules generally involves energetic transformations or a "transduction" between enthalpic contributions associated with attractive intermolecular interactions, as well as entropic contributions arising from an alteration of the configurational entropies of the molecules upon binding.[7,19] This compensation phenomenon creates uncertainties in the prediction of the entropy of association, ΔS. In particular, many studies aimed at enhancing the strength of

[a] *Materials Science and Engineering Division, National Institute of Standards and Technology, Gaithersburg, MD, 20899, USA.*
E-mail: fernando.vargaslara@nist.gov, jack.douglas@nist.gov
[b] *Departments of Physics and Molecular Biology & Biochemistry, Wesleyan University, Middletown, CT, 06459, USA*

molecular binding for applications, *e.g.*, drug discovery studies by pharmaceutical companies, have been based implicitly on the lock-and-key binding concept,[20] where binding is conceived solely in terms of the formation of complementary bonds between molecules having a fixed shape so that enthalpic interactions between the molecules are emphasized. Virtual screening studies of molecules,[21] and other computational methods based on optimizing enthalpy to enhance binding, however, have had limited success,[22] and it is now appreciated that changes in configurational entropy upon binding must be considered in any successful scheme for estimating the binding constants of macromolecules.[23] We believe that a systematic study of the enthalpy–entropy compensation (EEC) effect, mentioned above, should improve our capacity to predict and engineer binding constants for numerous medical and manufacturing applications.

Before initiating our study of the EEC phenomenon in the melting of duplex DNA, we point out that EEC is a widely occurring phenomenon that can arise from multiple molecular mechanisms. For example, Douglas *et al.*[24] have shown that the EEC effect in molecular binding can be analytically derived from a statistical mechanical model of the influence of interacting crowding molecules on associating proteins, providing insight into at least one mechanism of the EEC phenomenon. This mechanism of EEC was verified experimentally by Jiao *et al.*[25] and Sukenik *et al.*[26] Subsequent model calculations have indicated that EEC can also be derived analytically from other statistical mechanical models (molecular binding in telechelics, molecular binding to surfaces, and competitive binding of solvents to polymer chains) as a consequence of incorporating intermolecular interactions into the underlying reaction processes governing binding equilibrium.[27,28] The EEC effect has also been observed in the enthalpy and entropy of solvation energy of molecules and ions dissolved in water,[29,30] and corresponding statistical mechanical computations of the entropy and enthalpy of solvation upon adding molecules to associating fluids indeed give rise to EEC.[31] It is thus plausible that hydration can contribute to EEC in certain molecular binding processes as a thermodynamic consequence of solvent reorganization, as suggested before by Lumry *et al.*[32] and many others.[33,34] We note that our simulations of duplex DNA melting do not include explicit water, and thus the EEC effect that we observe in our simulations cannot be attributed to hydration. Further interpretations of EEC, along with many interesting examples drawn from molecular biology, are discussed by Pan *et al.*[35] and Starikov and coworkers.[36–39] The novelty of the present paper is that it considers a different mechanism of EEC from most previous studies. In particular, we are concerned about how changes in molecular rigidity of the bound molecules influence both the occurrence of approximate EEC in the binding of complex molecules with many internal degrees of freedom and with corresponding changes in the binding constant and cooperativity of molecular binding.

The specific goal of the present work is to understand what molecular parameters serve to influence the free energy parameters governing molecular association and the molecular mechanisms underlying EEC in the binding of complex molecules. We focus on duplex DNA melting in particular, since EEC has often been reported in this system and many molecular variables can be measured to gauge their influence on the entropy of association, ΔS. In particular, there are numerous measurements in which the chain length, salt concentration, and base sequence of DNA or RNA are varied to indicate that the enthalpy of association ΔH and ΔS vary in a proportionate fashion.[40] More broadly, EEC is found in diverse other molecular binding processes of significant biological interest such as drug–ligand binding,[41–44] protein folding and unfolding,[11,37] antibody maturation,[8,45–47] base-pair opening in RNA switches,[5,6,19] binding of HIV drugs to RNA,[48] binding of proteins to nanoparticles,[49] *etc.* EEC is clearly ubiquitous in the binding thermodynamics of biological macromolecules,[38,39,50,51] but what is the origin of this thermodynamic relationship? Recent experimental studies have suggested that EEC compensation might be a downstream consequence of changes in the rigidity of the associating molecules upon binding,[43,48,52–54] so we restrict our attention to how molecular rigidity influences molecular binding.

A previous computational work by Forrey, Douglas, and Gilson[52] considered the effect of varying molecular rigidity on the binding of two semi-flexible polymers using Brownian dynamics simulations where the EEC effect and changes in the energetic parameters governing molecular binding were found to be directly correlated with changes in chain rigidity, confirming previous experimental suggestions that molecular rigidity is a key variable in regulating the strength of molecular binding.[43,48,52–54] The present study builds on the work of Forrey *et al.* However, we utilize molecular dynamics simulations instead of Monte Carlo methods to investigate the effect of rigidity changes on molecular binding strength of the case of a pair of chain molecules having directional associative interactions, as found in DNA, RNA, proteins, and many other biomacromolecules. We alter the intrinsic chain rigidity both by changing the DNA chain length, and base pair interaction strength, *etc.*, and by introducing extrinsic constraints on duplex DNA, such as geometrical confinement to a slit geometry and the presence of ''crowding'' molecules in the environment that alter chain rigidity. We observe approximate EEC in all the systems that we simulate where the change in the entropy of association ΔS directly correlates with changes in the DNA duplex rigidity. Unexpectedly, however, we find that the signs of rigidity-induced shifts in ΔS and ΔH depend on whether the rigidity changes arise from changes in the intrinsic chain stiffness or from extrinsic constraints on the DNA.

Although the variation of molecular rigidity has a strong effect on the energetic parameters governing molecular binding, we find that the EEC effect is *imperfect*.[19] In particular, binding constants can be altered at a fixed T by varying molecular rigidity, although this effect is relatively weak in comparison to changes in ΔS and ΔH. This approach to overcoming strict EEC is exhibited in the molecular recognition of molecules of the immune system, such as antibodies. As antibodies progressively evolve to achieve a more specific binding to almost any antigen, they become more rigid; the mature antibody is relatively stiff

and binds with its partner in a lock-and-key complementary fashion.[8,45–47] This enhanced selectivity, of course, is critical to antibody function and we also obtain some insight into how this process works from a statistical mechanical perspective.

The paper is organized as follows. Section II describes the ssDNA molecular model and the computational methodology utilized in this manuscript. Section III presents experimental observations of EEC in the disassociation of dsDNA. Section IV presents the results from our calculations for the melting of dsDNA under different intrinsic and extrinsic conditions. Section V shows the numerical support that validates the EEC for the systems studied here, and we conclude in Section VI.

II. Computational model and methodology

A. DNA molecular model

We utilize a ssDNA coarse-grained model[55] widely used to study a variety of DNA-based systems such as the interaction between nanoparticles decorated with ssDNA,[56–58] the formation of Holliday junctions[59] and DNA hybridization in solution.[60] We select this model for its simplicity, which allows us to easily explore a vast range of model parameters and environments. In this molecular model of DNA, which we review for completeness here, we represent each ssDNA base by two "beads": one for the ssDNA phosphate–sugar backbone and one for the nitrogenous base; blue and green spheres depicted in Fig. 1. Below, we will refer to these coarse-grained DNA base structures as the backbone and nitrogenous beads. The backbone beads are connected by "springs" to form a chain (bead-spring model[61]) and we set the nitrogenous base identity (A, C, G, or T) in the interactions among the nitrogenous beads, so that only A and T, or G and C will interact attractively, and non-complementary bases interact only repulsively.

We next describe the molecular parameters in terms of this coarse-grained DNA model. First, the excluded volume interaction among all the particles that form our systems is achieved by using a Weeks–Chandler–Andersen potential (WCA), which is obtained by truncating and shifting the 12-6 Lennard-Jones potential (LJ) at its minimum $r_{\min} = 2^{\frac{1}{6}}\sigma$. Here, σ is the "bead" diameter defined as the average spacing between two connected nucleotides that form a ssDNA, $\sigma = 0.65$ nm.[58] Recent measurements of the ssDNA diameter by translocation of ssDNA chains through nanopores indicate that the ssDNA diameter is ≈ 0.8 nm, so that d_{ssDNA} is on the order of σ.[62] Each bead has a mass $m = 0.163$ kg mol^{-1}, which is 1/2 the average nucleotide mass.

The attractive interaction between two complementary bases (*i.e.* A green bead and T pink bead) is obtained by using smaller beads with diameter $0.35\sigma \approx 0.23$ nm with the LJ potential truncated at the cutoff separation $r_c = 2.5 \times 0.35\sigma \approx 0.57$ nm. These sizes were chosen such that the geometry of beads ensures one-to-one binding of complementary pairs, mimicking the lock-and-key base pairing of DNA. In this study, we only consider chains formed by poly(A) and poly(T) chains so that the attractive interaction strength ε (the Lennard-Jones energy parameter) between these bases is the same for all the pair bonds in the simulations of the present paper. In principle, we can simulate any base sequence by setting ε values for A–T and

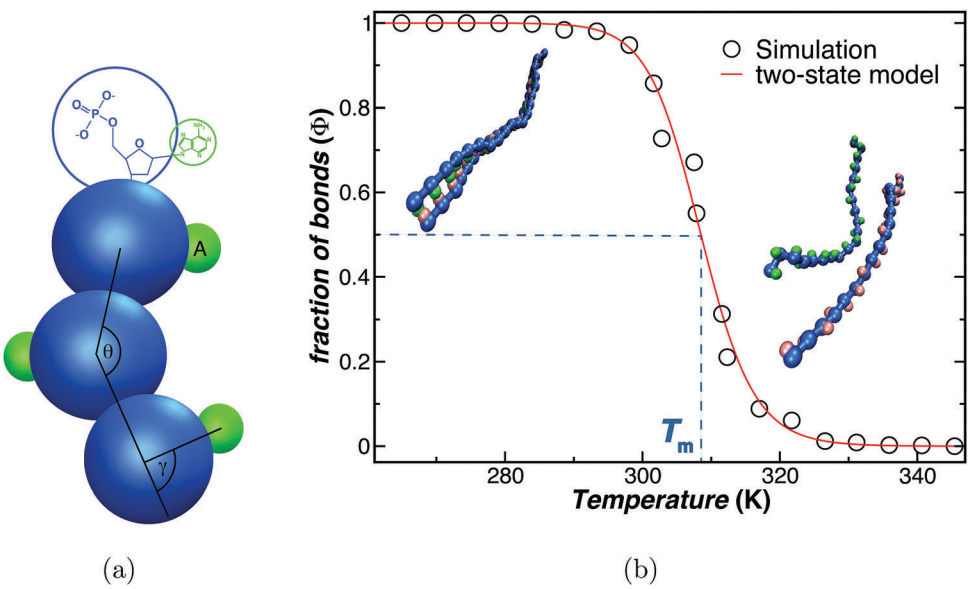

Fig. 1 (a) A coarse-grained representation of a ssDNA formed by 4 Adenine (A) bases. Here, each base is modeled by two force-sites, one for the phosphate–sugar backbone (blue bead) and the second one for the nitrogen base (small green bead). The blue beads are connected to form the chain. Additionally, each blue bead is connected to a small green one to represent the nitrogenous base adenine (A). (b) The fraction of bonds (Φ) that connects two complementary chains as a function of the temperature (T). The black circles represent the data and the red solid line is a fit to a two-state model (eqn (4)). The "melting temperature" T_m is the temperature at which only 1/2 of the bonds of dsDNA are intact, *i.e.*, $\Phi = 1/2$. The insets are typical configurations for two-complementary ssDNA, below and above T_m, left and right pictures, respectively. Here, one chain is formed by 20 A bases (blue-green chain) and the second one by 20 thymine (T) bases (blue-pink chain). From the two-state model, we obtain ΔH and ΔS for dsDNA melting.

G–C base pairs, where the ε values correspond to the enthalpy of melting for the base-pairs at 1 M NaCl, and pH = 7 reported in ref. 63. For this model, we consider ε = 19.67 kJ mol^{-1} as a representative value for the bonding interaction strength of complementary A–T nucleotides and ε = 24.0 kJ mol^{-1} for G–C base pairs.

The blue beads forming the backbone of the chain, and each blue bead with one small (green or pink) bead, that form a base (A or T) are connected by using a finitely extensible, nonlinear-elastic (FENE) anharmonic spring potential,

$$U_{\mathrm{FENE}}(r) = -\frac{k_{\mathrm{F}}R_0^2}{2}\ln\left[1-\left(\frac{r}{R_0}\right)^2\right], \quad (1)$$

where we fix the interaction strength k_{F} = 1397 kJ mol^{-1} nm^{-2} and the maximum bond length R_0 = 0.975 nm to model covalent bonds. To control the flexibility of the chain, adjacent connected beads interact with a three-body angular potential,

$$U_{\mathrm{bend}}(\theta) = k_{\mathrm{bend}}[1+\cos(\theta)], \quad (2)$$

with θ the angle defined by three consecutive blue beads along the chain, as shown in Fig. 1(a). By varying the bending stiffness k_{bend} in eqn (2), we can modulate the flexibility of the chains and explore the influence of chain stiffness on dsDNA melting, as described in Section IV B. Additionally, each small bead within the chain interacts with three neighboring beads that form the chain by,

$$U_{\mathrm{perp}}(\gamma) = \frac{k_{\mathrm{perp}}}{2}\left(\gamma-\frac{\pi}{2}\right)^2. \quad (3)$$

Here, k_{perp} = 1967 kJ mol^{-1} and γ is the angle formed by the center-to-center vector between the nitrogenous and backbone bead and the vector that connects two consecutive backbone beads, as depicted in Fig. 1(a). This potential, which is not varied in our simulations below, provides bond directionality and prevents two complementary neighboring backbone beads of the same chain from forming a bond. By choosing the bending stiffness value k_{bend} = 5.90 kJ mol^{-1}, we generate ssDNA chains formed by L = 20 T bases which have a persistence length of $\approx$2.4 nm at temperature T = 300 K. We take this ssDNA model chain as a reference system to compare among our calculations and the number of bases L as a dimensionless measure of DNA length.

No rigorous theory of melting exists, either for crystalline materials or duplex DNA, but many models have been introduced to describe the melting process.[64] For example, the recent theory of DNA melting by Peyrard–Dauxois–Bishop[65,66] emphasizes the anharmonicity of intermolecular interactions between the complementary binding base pairs and this model has much in common with earlier 1-dimensional spin models of DNA melting.[67–70] Other researchers have treated the binding and unbinding of ssDNA chains as a simple bimolecular association reaction at equilibrium,[71] which leads to a much simpler mathematical model of DNA melting. Both of these models are rather idealized, since the model of Peyrard–Dauxois–Bishop model the interacting dsDNA chains by a chain of 1-dimensional anharmonic oscillators and the bimolecular association model of DNA melting completely ignores the association–dissociation equilibria of the bases within duplex DNA upon approaching the melting point.

The melting model that we utilize for quantifying the results of our DNA molecular dynamics simulations data was derived as a leading approximation by Stillinger and Webber[72] as a model of crystal melting. This melting model assumes that the melting transition arises from the thermal generation of crystal point defects, *i.e.*, ''interstitials''. Stillinger and Webber also incorporated interaction effects between these defects[73] to account for cooperativity in the melting transition. We do not consider this more refined model since the simplified melting model of Stillinger and Webber provides an adequate approximation for all our simulation data. In future work, we plan to study the interaction of DNA ''bubbles'' composed of dissociated bases in the duplex[74] and the influence of the interactions of these defects on the cooperativity of DNA melting. Both crystal melting and DNA melting are often characterized as being first order transitions,[75] this attribute being more apparent in DNA melting when the chains are long.[76]

The simplified melting model of Stillinger and Webber is actually a widely utilized model in the biophysical community where it is known as the ''two-state'' model. In particular, this model is commonly utilized in quantifying and measuring data on protein unfolding and folding where a transition likewise exists between two molecular states, ''bound'' and ''unbound''.[32,77] In the context of DNA melting, Φ defines an ''order parameter'' for the DNA melting transition where Φ is described by the two-state thermodynamic relation,

$$\Phi(T) = \frac{1}{1+\exp[-\Delta F/(k_{\mathrm{B}}T)]}, \quad (4)$$

where $\Delta F = \Delta H - T\Delta S$ and $\Delta H = H_{\mathrm{u}} - H_{\mathrm{b}}$, $\Delta S = S_{\mathrm{u}} - S_{\mathrm{b}}$ are fitting parameters corresponding to the change in enthalpy and entropy between the unbound (u) and bound (b) states for the DNA chains, respectively, and k_{B} is the Boltzmann constant.

Fig. 1(b) shows how the average fraction of base bonds (Φ) within the chain changes when T is varied. Here, the melting temperature T_{m} in this model of melting is defined by the condition $\Phi \equiv 1/2$, which the two-state model directly relates,

$$T_{\mathrm{m}} = \frac{\Delta H}{\Delta S}. \quad (5)$$

In other words, the two-state description requires a specific EEC relation through the melting temperature. We emphasize, however, that the polymer chains do not dissociate until Φ is near zero so that the binding equilibrium involves base pairing and unpairing within the molecular complex rather than exchange of single-stranded chains between complexes. We strictly perform the data analysis of our simulations, based on eqn (4), in a temperature range where the single-stranded DNA molecules remain in contact (Fig. 2).

We utilize this two-state DNA melting model below to explore how altering intrinsic parameters of the two complementary chains, such as chain length (Section IV A), chain stiffness (Section IV B), or cohesive interaction strength (Section IV C)

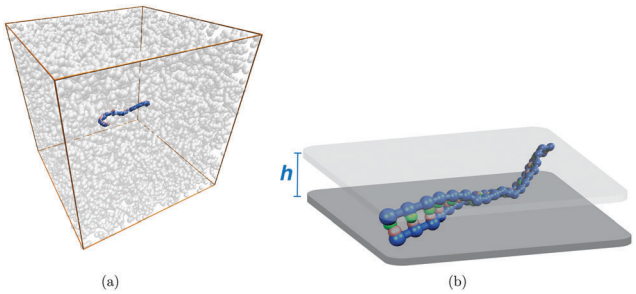

Fig. 2 Representative snapshots from the computer simulations for (a) a dsDNA interacting in a crowding environment and (b) a dsDNA under confinement to a slit geometry. In (a) the agent crowders are represented by a collection of chains (transparent silver chains) and in (b) the dsDNA chain confined by two rigid surfaces separated by a distance h. For both cases, the length of the dsDNA is fixed, L = 20 bp.

influences the thermodynamic variables T_m, ΔH, and ΔS. Section IV E explores the influence of molecular crowding in dsDNA binding by including chains "crowders" to interact with the dsDNA. Fig. 1(a) shows a representative configuration of a simulation box where a dsDNA is being packed with crowders (transparent silver chains). The crowders in this case are chains of length L_{crowd} = 20 or 50 of connected beads that interact repulsively with DNA; we vary the number of "crowder" molecules having the simulation box size fixed to change their volume fraction. In Section IV D, we study the influence of confinement on molecular binding by studying two complementary chains melt under confinement to a slit geometry of variable separation h (Fig. 1(b)), based on a model used previously to study dsDNA molecules under confinement.[78] The interaction between the parallel surfaces and the beads that form the chains is purely repulsive and is modeled by a 9-3 Lennard-Jones potential $U_{LJ}^{9\text{-}3}(r)$,

$$U_{LJ}^{9\text{-}3}(r) = \varepsilon_s\left[\frac{2}{5}\left(\frac{\sigma_s}{r}\right)^9 - \left(\frac{\sigma_s}{r}\right)^3\right], \quad r < (2/5)^{1/6}\sigma_s, \qquad (6)$$

where the bead–wall distance parameter σ_s = (0.65 or 0.228) nm for the interaction between the surface and backbone and nitrogenous bead, respectively, and ε_s = 19.67 kJ mol^{-1}.

We study these systems by using molecular dynamics simulations for NVT ensembles in the T range $(270 \lesssim T \lesssim 430)$ K. To control T, we use the Nose–Hoover method.[79,80] We integrate the equations of motion by using the Large-scale Atomic/Molecular Massively Parallel Simulator (LAMMPS),[81] along with the rRESPA multiple time-step algorithm[82] and periodic boundary conditions.[83] For melting studies, we start by performing simulations at low temperature to ensure the connectivity of the two ssDNA chains. We next gradually increase T of the systems to reach the desired final temperature. Then, we generate 10 copies of each system by randomizing their initial velocities and we let the systems run until they reach the thermal equilibrium. We finally collect statistics for $>10^7$ time steps Δt of each system, with $\Delta t = \sigma\sqrt{m/\varepsilon} = 1.875 \times 10^{-12}$ s.

B. Characterizing the rigidity of ssDNA and dsDNA chains

Since we argue that changes to the stiffness of DNA are critical for understanding the compensation behavior, we first characterize the rigidity of DNA in both single and double-stranded forms. The problem of characterizing the rigidity of DNA is complicated by the complexation between the ssDNA chains, which makes the stiffness of dsDNA depend on the stiffness of the individual DNA strands and the interaction strength between the chain bases. As with crystalline materials, the stiffness can be expected to change sharply as the duplex DNA begins to melt; non-uniformity in base sequence gives rise to variation in the local binding strength in the molecules that also leads to a variation in the stiffness along the DNA chain that can cause kinking and bending of the duplex DNA. These complexities cannot be adequately addressed in the simple worm-like chain model and we thus consider alternative rigidity measures. Different rigidity measures should also be useful in studying molecular binding in systems other than duplex DNA. Specifically, we quantify the chain "stiffness" for DNA below, by computing the persistence length (l_p) of both ssDNA and dsDNA. In particular, l_p for the dsDNA can be experimentally obtained from direct imaging techniques, and from a variety of scattering techniques such as neutron scattering.

Following common experimental practice,[84] the persistence length (l_p^{ss}) of single stranded DNA (ssDNA) can be estimated as the average projection of the chain end-to-end distance $\mathbf{R}_e$ on the first bond of chain $\mathbf{l}_1$,

$$l_p^{ss} = \langle \mathbf{R}_e \cdot \mathbf{l}_1 \rangle / \langle l_1 \rangle. \qquad (7)$$

We prefer this definition of persistence length since it does not assume the validity of the worm-like chain model of semi-flexible polymers in dilute bulk solutions,[85] which neglects excluded volume interactions and assumes that the polymer can be described in terms of macroscopic continuum semi-flexible filaments. We know from our previous work on DNA under geometrical confinement that although the worm-like chain model provides a reasonable model of the mean size $\langle R_e^2 \rangle$ of semi-flexible polymers,[86] it can provide only an inadequate description of DNA subject to confinement[78] and below we find further evidence for the limited applicability of the worm-like chain model.

For example, it is frequently assumed, based on the worm-like chain model, that l_p^{ss} can be directly related to the rigidity of the individual DNA molecules as, $l_p^{ss} = \kappa_{ss}/k_BT$, where κ_{ss} is the ssDNA bending rigidity. Based on this thinking, we initially investigated κ_{ss} as an appropriate measure of DNA rigidity for our binding studies, but the implementation of this idea led to difficulties that were anticipated by recent theoretical investigations of semi-flexible polymers. In particular, Lipowsky and coworkers[87] found that the often assumed relation, $l_p^{ss} = k_{ss}/k_BT$, does not hold when polymers are flexible due to the neglect of thermal fluctuation effects. Instead, l_p^{ss} is predicted to equal, $l_p^{ss} = \delta l_p^{ss} + \kappa_{ss}/k_BT$, where the fluctuation contribution to the persistence length, δl_p^{ss}, is a constant whose magnitude can be appreciable. For highly stiff chains, this term vanishes, $\delta l_p^{ss} \approx 0$, so that the standard worm-like chain model is applicable for relatively rigid structures, such as carbon nanotubes and tubulin. However, ssDNA is a highly flexible polymer and this

fiber assumption does not apply. We have confirmed the existence of the predicted[87] fluctuation contribution δl_p^{ss} (see Appendix A), which allowed us to determine κ_{ss}. Nonetheless, the determination of δl_p^{ss} is an obvious complication in estimating the "rigidity" of real single stranded DNA so we looked for an alternative measure of rigidity that is more convenient for both experimental and simulation studies of molecular binding. The persistence length of dsDNA has the advantages of being accessible by direct imaging and a negligible fluctuation contribution to the persistence length δl_p because of the significant rigidification accompanying duplex formation, a phenomenon discussed extensively below. We thus take κ_{ds} of duplex DNA as our fundamental measure of DNA molecular rigidity in relation to our study of how molecular rigidity influences the energetic parameters governing duplex DNA melting. In the next section, we define l_p for duplex DNA and contend with complications that arise from the fact that κ_{ds} changes appreciably with T as duplex DNA approaches its melting temperature, T_m. This problem is resolved by determining the magnitude of $\kappa_{ds}(T)$ for $T \ll T_m$ where it becomes a constant, κ_{ds}^0. This measure of the bending stiffness of dsDNA will play a significant role in our discussion below.

The persistence length of double-stranded DNA (l_p) can be defined as the average persistence length of the intertwined ssDNA chains forming the duplex DNA,

$$l_p = (l_{p1}^{ss} + l_{p2}^{ss})/2. \quad (8)$$

Fig. 3(a) shows a representative calculation for the persistence length of dsDNA (black circles) and ssDNA (red squares) as a function of T. We see that l_p decreases rather abruptly on approaching T_m, and on melting, recovers the expected value for single strands, an effect that is not normally accounted for in models of duplex DNA stiffness. Although the origin of this significant T dependence is rather obvious, *i.e.*, the DNA duplex melts, there are surprisingly few studies on this phenomenon. Recently, this problem has attracted interest, however, and Geggier *et al.*[88] experimentally observed an appreciable change in l_p with T that is in qualitative accord with our simulations. Moreover, the introduction of appropriate reduced variables allows us to make a quantitative comparison between these experimental and simulation estimates of l_p. In particular, we normalize $l_p(T)$ by its value near T = 236 K, a value that is well below T_m, and we define the reduced temperature as T/T_m and the inset to Fig. 3(a) shows a direct comparison between our simulation results for $l_p(T)$ and the experiments reported by Geggier *et al.*[89] In this plot, we use the experimental estimate T_m = 326 K determined by Nagapriya *et al.* for a similar type of plasmid dsDNA[90] investigated by Geggier *et al.* We see that l_p^{ss} varies relatively slowly with T and has a much smaller magnitude than l_p.[91] It is evident that molecular unbinding gives rise to a large change in DNA rigidity that depends rather strongly on T near T_m.

For the relatively stiff duplex DNA molecular complex, there is a direct relationship between the persistence length and the rigidity parameter, $l_p(T) = \kappa_{ds}(T)/k_BT$, which greatly simplifies our quantification of molecular rigidity. Fig. 3(a) shows $\kappa_{ds}(T)$ for a dsDNA (black circles) and a ssDNA (red squares) as a function of k_BT. For the dsDNA case, in the low T regime ($T \ll T_m$), κ_{ds}^0 is constant at low T where the duplex DNA is fully hybridized (blue line in Fig. 3(b)). The abrupt transition in κ_{ds} upon approaching the melting transition can be expected in any fiber forming system near its "melting transition", *e.g.* actin, tubulin, amyloid fibers, and many other biological structures of fundamental interest.[92,93]

Within the conceptual framework of the continuum worm-like chain model, the abrupt change in κ_{ds} as a function of T can be attributed to a decrease in the flexibility parameter $\kappa_{ds} = EI$, where

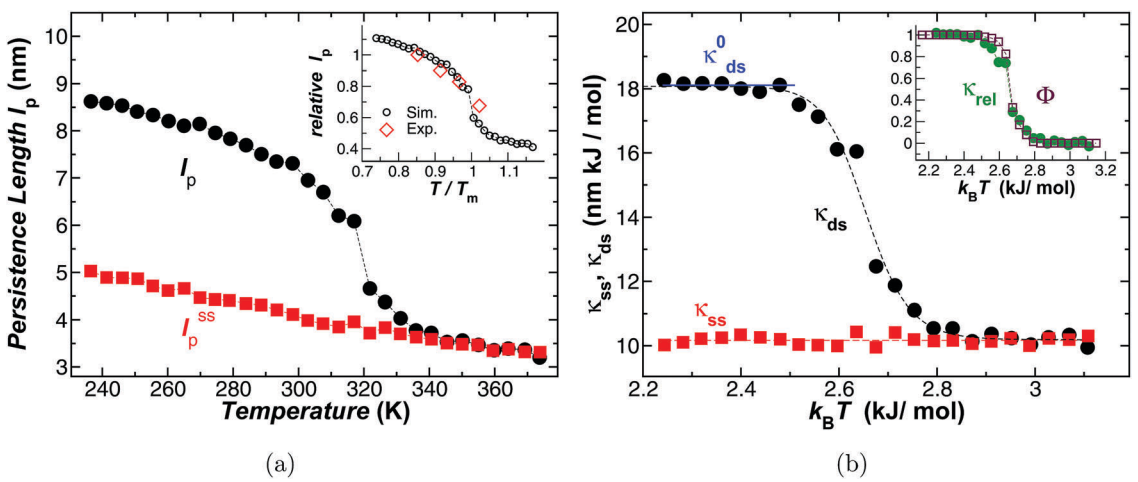

Fig. 3 The left panel shows an example calculation for the persistence length (l_p) for a dsDNA chain (black circles) and a ssDNA chain (red squares) as a function of the temperature T. The inset in this figure is a comparison for the relative l_p for the dsDNA data presented in the main figure (black circles) and experimental results (red solid diamonds) obtained from ref. 88. The right panel shows the fraction of bonds that connect the two ssDNA Φ (green diamonds) and the relative persistence length l_p (blue triangles) given by eqn (9) as a function of the temperature. The change in DNA rigidity is directly related to the number of bonds that connect the two ssDNA chains.

E is the Young's modulus of the fiber and I is the geometrical moment of inertia. For rods having a circular cross section equals, $I = (\pi R^4)/4$, where R is the cross-sectional radius of the fiber,[94] more generally, I is highly sensitive to fiber cross-section shape. For an ideal I-beam shape, which is a reasonable approximation for dsDNA, this quantity can be as large as a factor of 10 greater than for a rod of the same cross-sectional area.[95,96] This emergent rigidity of self-assembled fibers also depends on the number of chain molecules in the self-assembled fibers. For dense bundles of chains, we might expect this amplification factor to rise with the fourth power of the number of chains (N),[94] reflecting the growth of the cross-sectional area moment I, but in hollow fibers such as found in DNA "origami" nanotubes, the variation is observed to be $\kappa \sim N^2$,[17] and in ribbon-like fibers, as often found in amyloid fibers, κ scales nearly linearly with N.[97] Moreover, the rigidity of self-assembled fibers depends on the strength of the intermolecular interaction ε between the chains so that other molecular factors than fiber geometry are important. We next quantify this interaction effect on the rigidity of dsDNA.

It is evident from Fig. 3(a) that the largest contribution to duplex DNA rigidity derives from inter-base interactions, so it is natural to seek a relationship between the rigidity of dsDNA and the extent of melting of complex, which can be estimated by a variety of experimental techniques. In particular, we define $\delta\kappa(T)$,

$$\delta\kappa(T) = \frac{\kappa_{ds}(T) - \kappa_{ss}(T)}{\kappa^0_{ds} - \kappa_{ss}(T)}, \tag{9}$$

as a measure of the rigidity change of DNA that derives from duplex formation. By definition, this quantity varies from 1 at low temperature to 0 at high temperature so that $\delta\kappa$ also provides a measure of the extent of duplex DNA melting. This physical interpretation of $\delta\kappa$ can be appreciated from the inset in Fig. 3(b), where we directly compare $\delta\kappa(T)$ to the average fraction of bonded bases in the dsDNA Φ. In particular, we find the quantitative relationship between Φ and $\delta\kappa$,

$$\delta\kappa(T) \approx \Phi(T). \tag{10}$$

Eqn (10) implies that we can estimate the temperature dependent persistence length for dsDNA from κ^0_{ds}, Φ, and l^{ss}_p. This type of relationship was suggested by Douglas and coworkers in ref. 98 in connection with estimating the shear modulus of thermally reversible gels formed by self-assembly. We note that the two-state model approximation to the stiffness of materials seems to provide a good phenomenological description of diverse materials, ranging from gels, polymer nanostructures, foods, and other complex disordered solids.[98,99]

For molecules exhibiting a greater chemical heterogeneity than duplex DNA, the persistence length and bending rigidity do not provide useful measures of molecular rigidity because chain rigidity varies locally within the molecule. We then need experimentally accessible local measures of molecular rigidity since only part of the molecule may be directly involved in molecular binding. In particular, the presence of local relatively rigid or soft elements in the molecule can influence rigidity globally, leading to highly non-trivial allosteric effects on molecular binding[100] and we would also like to quantify this phenomenon within the same conceptual framework as the present paper. The problem of quantifying changes in molecular rigidity in relation to changes in binding energetic parameters is a fundamental challenge in biophysics.[45] We briefly address this general problem in the next section, although most of our analysis of dsDNA will employ k^0_{ds} as the basic rigidity measure in our development below. In Appendix B, we discuss alternative estimates of molecular rigidity that should be useful in a more general context of molecules where rigidity is not readily described by the persistence length.

III. Experimental observation of enthalpy–entropy compensation in DNA duplex melting

The dissociation of duplex DNA has been widely studied by the scientific community. Experimental measurements of T_m, ΔH_{total}, and ΔS_{total} for DNA chains having different sequences, length chains, and solution chemistry have been reported.[13,14,101] In particular, the experimental study performed by Manyanga *et al.*[101] provides important information about the thermodynamic variables relating the dissociation of dsDNA, as determined from spectroscopic and calorimetric measurements. Manyanga *et al.* find a good correlation between ΔH, ΔS, and T_m, and we review these observations to define the nature of the EEC phenomenon and our notation. First, we reproduce some of their results in Fig. 4. Panel (c) shows the change in enthalpy ΔH as a function of the change in entropy ΔS for the melting of short DNA chains having different chain sequences and chain lengths. The symbols in this figure correspond to the data and the dashed line is a guide to the eye. (This work, ref. 54, should be consulted regarding details of the measurement and experimental uncertainties.) We see a near proportional relation between ΔH and ΔS, which in the literature is referred to as "enthalpy–entropy compensation" (EEC). (Remarkably, EEC is also observed locally within the duplex DNA for specific groups of bases within the nucleic acid sequence as found in riboswitches.[13]) Another common way of representing this kind of EEC plot involves multiplying ΔS by a reference temperature, which is frequently taken to be the room temperature, T_R = 300 K, see panel (b) in Fig. 4. As suggested by the two-state description eqn (5), a more convincing form of EEC can be found by multiplying ΔS by T_m, as illustrated in Fig. 4(c). Since EEC in the sense is an exact consequence of the two-state nature of molecular binding, we are actually observing a mathematically trivial effect of enthalpy–entropy compensation that arises in almost any thermodynamic transition or binding process. On the other hand, the factors that control the movement along this line through the variation of ΔS, ΔH, and T_m are far from trivial. We next determine the molecular factors that influence these basic binding parameters.

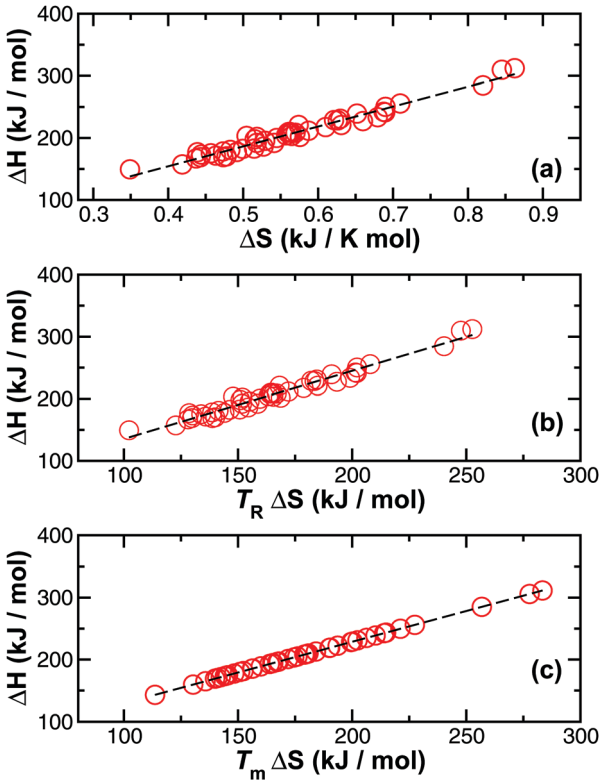

Fig. 4 In panel (a), the change in enthalpy ΔH as a function of the change in entropy ΔS for experimental systems. The data were obtained from ref. 101. In panel (b), ΔS is multiplied by the room temperature T_R = 300 K. In panel (c), ΔS is multiplied by the dsDNA melting temperature T_m obtained from an independent measurement.

IV. Influence of molecular parameters on the melting of duplex DNA

A. Influence of chain length L on duplex DNA binding energetic parameters

In order to design new materials based on DNA (such as DNA origami), it is important to know how the structural parameters of the ssDNA, such as the length of the DNA segment and base composition, affect the thermodynamic stability of the resulting assembly. For this reason, we explore the influence of chain length L on dsDNA melting using the molecular model described in Section II. First, we must clarify how changing the length L of the dsDNA directly influences the rigidity of the complexes, an effect not anticipated from the continuum worm-like chain model of DNA. Fig. 5 shows the effect of changing L on the persistence length over the range of L and for a range of temperatures fully encompassing the DNA melting transition. We find that all our l_p data as a function of L for various T can be described an the approximant inspired by renormalization group cross-over theory,[102]

$$l_p/l_p^{\infty} = \frac{(L/L_c)^{\alpha_L}}{1+(L/L_c)^{\alpha_L}}, \qquad (11)$$

where L_c and l_p^{∞} are fitting parameters which depend on T, and α_L = 2 is fixed for all the data presented in this figure. Recent experimental estimates[103] and atomistic simulation estimates[104] of l_p as a function of DNA chain length L show the same trend and these data are also included in Fig. 5, although the chain length in the experimental measurements is much larger than those considered in the present work. Nevertheless, we can compare our simulation results to the experimental estimates if we employ the reduced variables, l_p/l_p^{∞} and L/L_c. First, we note that we have the simple relation $l_p/l_p^{\infty} = \kappa_{ds}^0/\kappa_{ds}^{\infty}$, at low temperature, where κ_{ds}^{∞} is the rigidity parameter in the long DNA chain length limit. A qualitatively similar variation of l_p with fiber length has been observed in self-assembled tubulin fibers and amyloid fibers, so the effect seems to be rather general for fibers formed by self-assembly.[105] A chain length dependence on l_p also arises in our chain model of ssDNA, so that this effect does not exclusively derive from the interaction between the DNA chains within duplex DNA. Evidently, we are seeing another fluctuation effect that is not anticipated by the continuum worm-like chain model.

Fig. 6(a) shows the fraction of bonds Φ between the bases within the duplex varying with T for dsDNA chains formed with L = (10, 15, 20, 30, 40, or 50) complementary base pairs (T–A). The symbols in this figure correspond to the data and the lines are fits to eqn (4). From this plot, we extract T_m, the enthalpy, and the entropy of dissociation, ΔH, and ΔS. We show these thermodynamic parameters as a function of the chain length L in Fig. 6(b), (c), (d), respectively. Based simply on the fact that more nucleotide links must be severed as we increase L, ΔH and ΔS should increase with length. We indeed find that T_m, ΔH, and ΔS become larger with increasing L, but the rate of increase but these changes saturates in the limit of long and rigid chains. There is evidently a strong correlation between changes in ΔH, ΔS, and chain rigidity, which is the focus of our discussion below.

B. Influence of intrinsic stiffness of DNA on duplex DNA binding energetic parameters

The stiffness of DNA can be altered by changing the DNA sequence[89] or solution conditions such as by varying the salt concentration[106] or by the binding of protein or other molecules to DNA. Such rigidity changes are important for biological activity. In particular, changes in the flexibility of actin[12] and hemoglobin binding metal ions have been shown to be highly correlated with the adaptation of organisms to new environments.[23,107] To directly investigate the influence of chain stiffness, we modify the bending stiffness parameter k_{bend} in eqn (2) to create model "flexible", "semi-flexible", and "stiff" chains. We then explore how chain stiffness affects the thermodynamic stability of duplex DNA. Fig. 7 shows how the bending energy of the duplex DNA at low T, κ_{ds}^0, depends on k_{bend}. The relation between κ_{ds}^0 and k_{bend} is not linear and there is no obvious trend towards saturation, as found when L is increased.

Fig. 8(a) shows the fraction of bonds Φ as a function of T for chains having different flexibilities, while Fig. 8(b), (c), and (d) show T_m, ΔH, and ΔS, respectively, as a function of k_{bend}. Evidently, T_m, ΔH, and ΔS become larger as k_{bend} becomes larger, so that DNA complexes composed of stiffer chains are

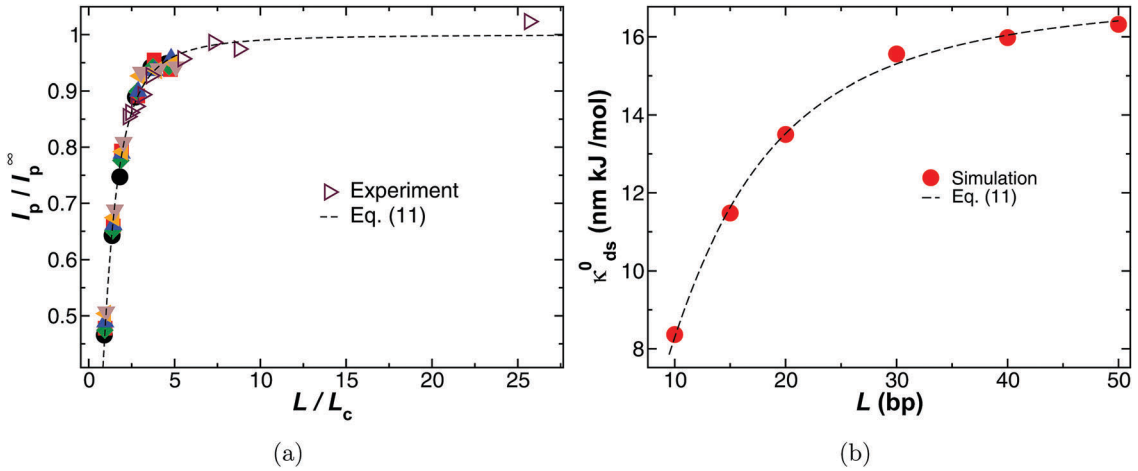

Fig. 5 In (a), the normalized persistence length of dsDNA chains having L = (10, 15, 20, 30, 40, or 50) complementary base pairs (bp) (T–A) as a function of its normalized chain length (see eqn (11)). Here, the normalization factors l_p^∞ and L_c depend on temperature. The empty symbols represent the data calculated in this work and the solid symbols are experimental measurements obtained from ref. 103. The line is a fit to eqn (11). In (b), κ^0_{ds} as a function of L, where we find κ^0_{ds} reaches a saturation value. The values of k_{bend} = 5.90 kJ mol^{-1} and ε = 19.67 kJ mol^{-1} are fixed in these simulations.

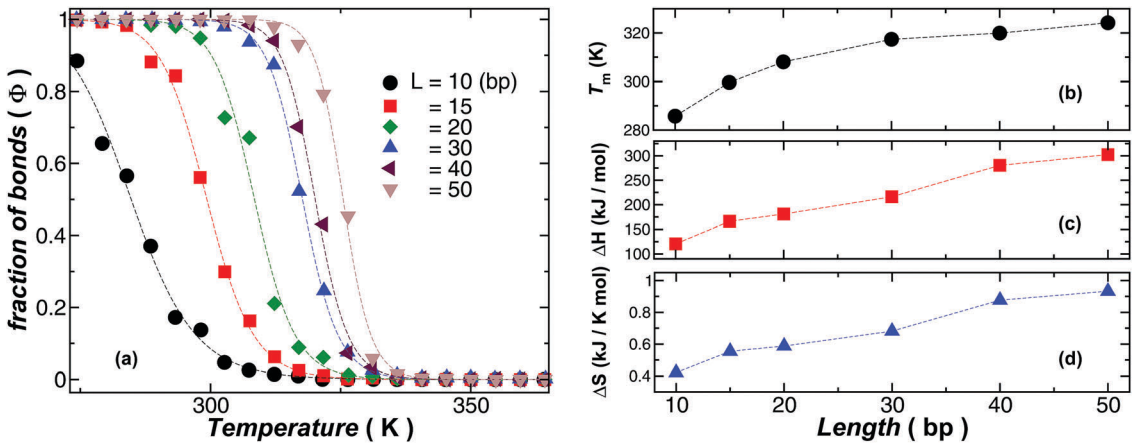

Fig. 6 In (a), the fraction of bonds as a function of temperature for the disassociation of dsDNA chains having L = (10, 15, 20, 30, 40, or 50) complementary base pairs (bp) (T–A). The symbols represent the data and the lines are fits to eqn (4). From this plot, we extract T_m, ΔH, and ΔS of dissociation and we plot these variables as a function of the chain length in (b), (c), (d), respectively. We find that T_m, ΔH, and ΔS become larger with increasing L.

more thermodynamically stable against melting, other factors being fixed. We note this situation is not comparable to changing persistence length by changing salt concentration, since the addition of salt also affects electrostatic screening, which has a competing effect on T_m. Above, we found that the stiffness parameter k^0_{ss} varies roughly linearly with k_{bend} (see inset of Fig. 7) so that k^0_{ds} then varies non-linearly with k^0_{ss}.

In the next section, we show that the variation of the base binding energetic parameter ε also leads to a rigidification of the DNA when ε becomes larger, increasing the change in ΔH and ΔS. Recent experimental studies have indicated that the mutual interaction strength of molecules in self-assembled molecular fibers such as amyloid fibers, tubulin, actin, *etc.* is as important as the fiber cross-sectional shape and diameter in determining the molecular rigidity of the resulting fiber assembly.[97]

C. Influence of the interaction strength ε on binding energetic parameters

DNA usually interacts with other species of molecules, intercalating dyes, ions and/or counterions, molecules, *etc.*, and these interactions can collectively be expected to influence the DNA binding strength of the bases ε, so that ε subsumes all the complexity of the intermolecular interactions influencing T_m, ΔH, and ΔS. Although values of ε are normally determined under fixed thermodynamic conditions, we consider ε to be a variable to gauge the influence of this fundamental interaction variable on dsDNA stability. Varying ε also provides a mean field indication of how varying the relative A–T and G–C content in duplex DNA influences the dsDNA stability, if we consider ε to be a compositionally weighted average over the base sequence, although we consider a range larger than accessible by simple compositional changes of sequence (Note range of epsilon in Fig. 9).

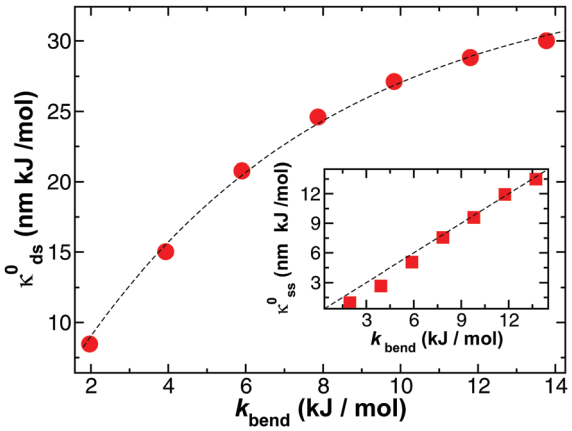

Fig. 7 The intrinsic rigidity for dsDNA κ_{ds} as a function of k_{bend}; the symbols correspond to the data and the dashed line is a guide to the eye for a L = 20 bp with a bonding interaction strength ε = 19.67 kJ mol^{-1}. Here, we vary the chain stiffness parameter, k_{bend}, to generate flexible, semi-flexible and stiff chains.

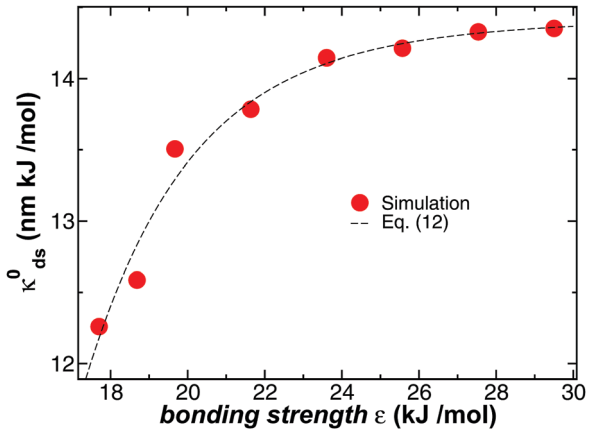

Fig. 9 The intrinsic rigidity κ^0_{ds} as a function of ε. The symbols correspond to the data and the dashed line is a guide to the eye for a L = 20 bp chain.

Varying ε leads to effects that do not exist in condensed matter systems in which chain connectivity is not present, since the connectivity and bending energy introduce independent energy scales. In particular, changing ε might be expected to have an equivalent effect to altering of temperature, as found in simple structures-less fluids such as Lennard-Jones fluids, but varying ε alters the DNA rigidity as found in shear modulus of bulk materials,[108] which is accompanied by non-trivial changes in both ΔH and ΔS. Moreover, we see in Fig. 10 that both ΔH and ΔS increase progressively with the base binding strength ε, but this trend saturates at large ε, as we found before with increasing L.

We quantify this effect by showing that the variations of κ^0_{ds} at fixed ε follow a similar trend as found before for κ^0_{ds} as a function of L and, accordingly, we use the same type of cross-over function to describe the variation of κ^0_{ds} with ε,

$$\kappa^{ds}_{ds}/\kappa^{\infty}_{ds} = \frac{(\varepsilon/\varepsilon_c)^{\alpha_\varepsilon}}{1+(\varepsilon/\varepsilon_c)^{\alpha_\varepsilon}}, \qquad (12)$$

where κ^{∞}_{ds} = 14.4 nm kJ mol^{-1}, ε_c = 14.1 kJ mol^{-1}, and α_ε = 7.35 (See Fig. 9 for comparison of our simulation results to eqn (12)). Increasing the rigidity of duplex DNA by either varying the chain length L or the intermolecular binding strength ε influences the intrinsic rigidity of the DNA duplex and correspondingly leads to an increase of ΔH and ΔS, following a (by now) general pattern. Below, we show that ΔH and ΔS sharply increase in magnitude as κ^0_{ds} approaches it limiting value κ^{∞}_{ds}, so this limit has great significance in modulating the energetic parameters governing molecular binding. The variation of ε along the chain backbone causes the chain stiffness to correspondingly vary locally, leading to a bending of the chain.[109,110] We next consider how external constraints on duplex DNA, such as geometrical confinement and the presence of crowding molecules, influence these basic binding energetic parameters.

D. Influence of geometrical confinement on binding energetic parameters

Many developing methods of rapid DNA sequence determination include confining DNA to small pores or other highly confined

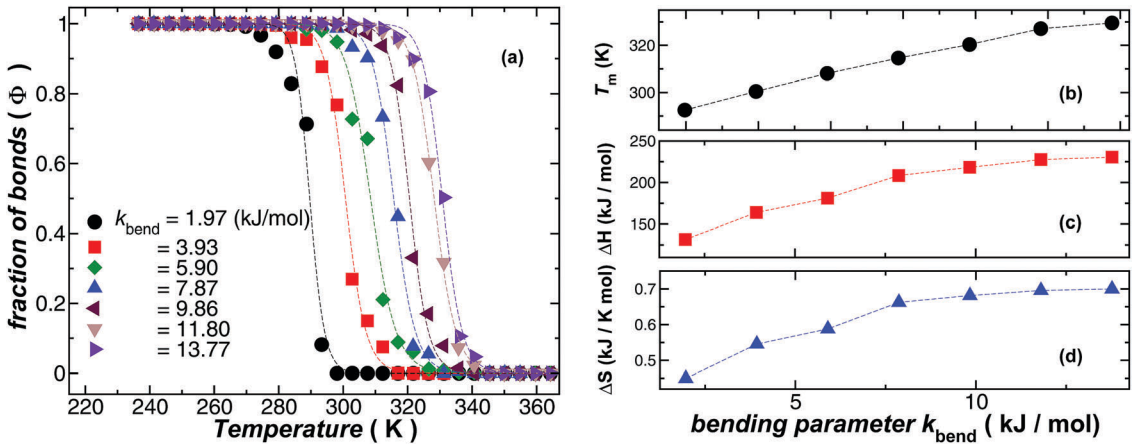

Fig. 8 In panel (a), the fraction of bonds (Φ) as a function of temperature (T) for the disassociation of a dsDNA chain having 20 complementary bases. The symbols are the data and the lines are fits to eqn (4) from where we extract T_m, ΔH, and ΔS, which are plotted as a function of k_{bend} in panels (b), (c), and (d) respectively. We find that the stiffer chains are more thermodynamically stable.

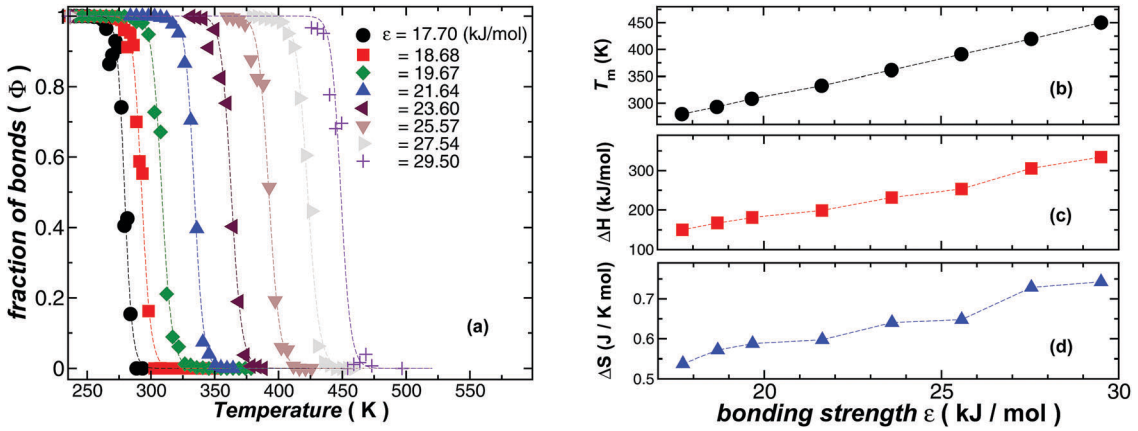

Fig. 10 The fraction of bonds (Φ) as a function of temperature (T) for the disassociation of a duplex DNA having 20 complementary bases and fixed intrinsic rigidity. The different sets of data in panel (a) represent chains interacting with different binding strengths, ε. In general, T_m, ΔH and ΔS increase with higher interaction strength, as we can see from panels (b), (c), and (d), respectively.

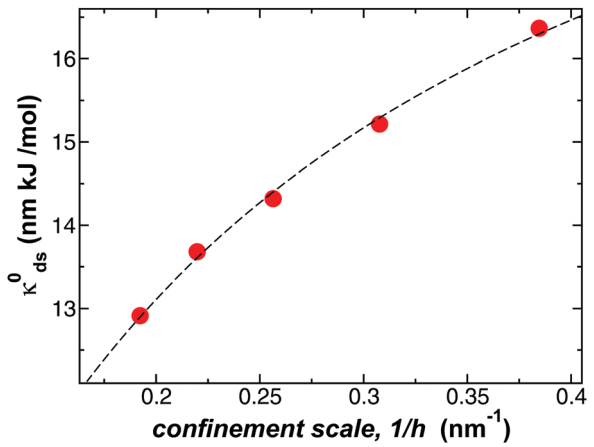

Fig. 11 The intrinsic rigidity κ^0_{ds} as a function of the degree of confinement $1/h$. The symbols correspond to the data and the dashed line is a guide to the eye. The calculations are for a dsDNA chain having L = 20 bp and fixed ε = 19.67 kJ mol^{-1} and k_{bend} = 5.9 kJ mol^{-1}.

geometries so that the study of the thermal stability of dsDNA under confinement has practical as well as scientific interest.[111] Fig. 11 shows the effect of varying the confinement scale h on the rigidity of duplex DNA, κ^0_{ds}. Correspondingly, Fig. 12 shows $\Phi(T)$ for chains between two parallel repulsive surfaces separated by distances h = (2.60, 3.25, 3.90, 4.55, or 5.20) nm. The symbols represent the data and the lines are fits to eqn (4). As with changes in the intrinsic rigidity, T_m, ΔH, and ΔS all vary as h is varied, other molecular variables being fixed (Fig. 12). Confinement between parallel plates with repulsive interactions then stabilizes the duplex DNA against melting. This is the well known "crowding" phenomenon. We next consider the related case where the crowding effect derives from surrounding molecules that are not directly involved in molecular complexation.

E. Influence of crowding molecules on duplex DNA binding energetic parameters

The concentration of macromolecules in cells is rather large ($\approx$40% by volume) and it is generally appreciated that this must greatly influence the energetic parameters of binding processes in such a complex environment.[112,113] It has been established that this crowding effect plays an essential role in regulating numerous biological processes that are essential for living systems. For example, crowding has been implicated as the primary factor in the organization of the cytoplasm[114] and the cell nucleus[4,115] of animals and in the regulation of nuclear function.[116,117] Crowding is also implicated in the nucleoid organization of DNA in bacteria.[118] We may also expect that the use of crowding agents in the fabrication of new materials to become a powerful tool in synthetic materials development. We next investigate how model crowding agents (*i.e.*, flexible polymers having repulsive interactions with the dsDNA) affect the thermal stability of dsDNA. The conventional approach to this type of intermolecular crowding interaction on molecular binding, pioneered by Minton,[112,119–121] is to treat crowding as being a simple consequence of excluded volume interactions between the polymer (treated as an effective hard sphere) and the associating molecular species, which is also normally treated as an effective hard sphere. In our approach, we are concerned with the fact that the crowding molecules and the binding species both have thermally active internal degrees of freedom that can respond to changes under thermodynamic conditions and upon intermolecular binding. This leads to a many-body coupling between the internal degrees of freedom of the crowding and binding species, where this coupling modulates the energetic parameters governing molecular binding. We next consider how this subtle crowding interaction works in our DNA molecular model (Fig. 13).

Fig. 13 shows the effect of increasing the concentration of crowding molecules on the molecular stiffness parameter, κ^0_{ds}. Correspondingly, Fig. 14(a) shows $\Phi(T)$ for chain "crowders" represented by polymer chains having a length of L = 20 beads and having purely repulsive interactions with dsDNA. The volume fraction of crowding molecules ϕ is changed by adding more crowding chains to the simulation box of fixed volume. The symbols represent the simulations data and the lines are

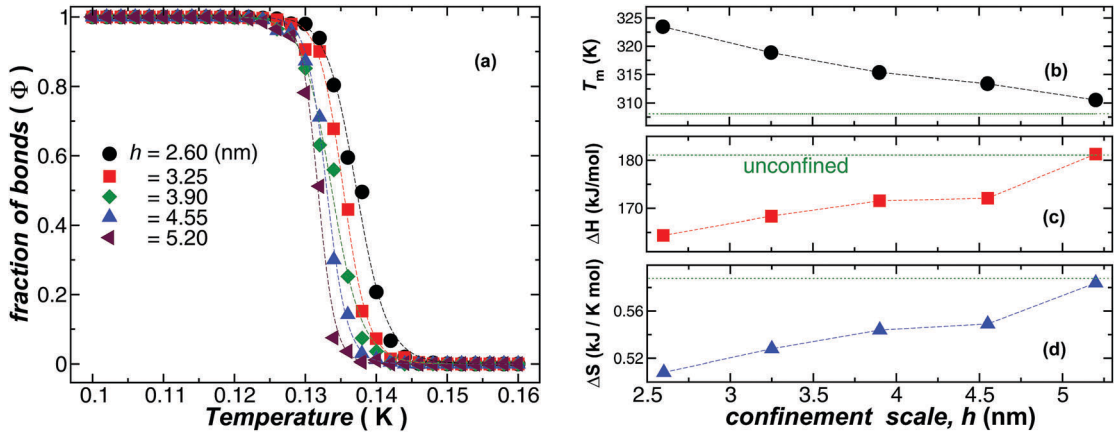

Fig. 12 The fraction of bonds (Φ) as a function of temperature (T) for the disassociation of duplex DNA chain having L = 20 bp interacting between two parallel slits separated by a distance gap, h = (2.60, 3.25, 3.90, 4.55, or 5.20) nm. The reduction of available space for the dsDNA makes it more stable, T_m gets larger for more confined chains. On the other hand, ΔS is smaller for more confined chains due to the reduction of space available for the chain, and ΔH seems to track ΔS.

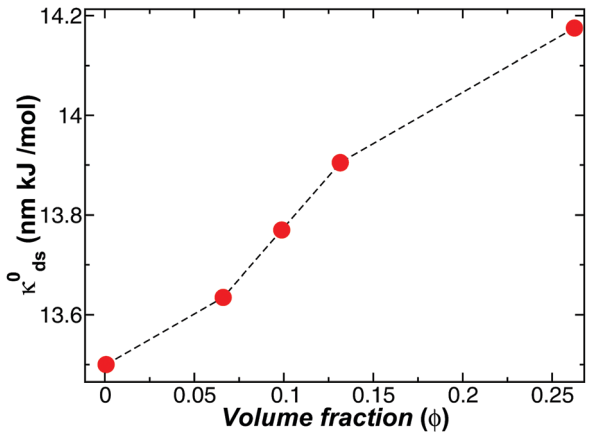

Fig. 13 The intrinsic rigidity κ_{ds}^{0} as a function of ϕ. The symbols correspond to the data and the dashed line is a guide to the eye for a L = 20 bp chain.

fits to eqn (4). Fig. 14(b), (c), (d), show T_m, ΔH, and ΔS as a function of ϕ for our reference duplex DNA model. As in the case of confinement between two repulsive walls, the crowder molecules reduce the number of accessible configurations of the dsDNA, thus altering the thermodynamic binding parameters. In particular, T_m increases for higher ϕ, but ΔH and ΔS become smaller at higher ϕ. We emphasize that the presence of a non-specific attractive interaction between the crowding molecules and the associating species can greatly influence the effect of the crowder molecules on molecular binding,[24,25,113] but such non-specific attractive interactions between the binding species and the crowder molecules are not considered in the present work. An attractive interaction between the duplex DNA and confining boundaries[78,122] can be expected to likewise alter ΔH and ΔS. The influence of these attractive interactions is discussed below in connection with shifts in T_m.

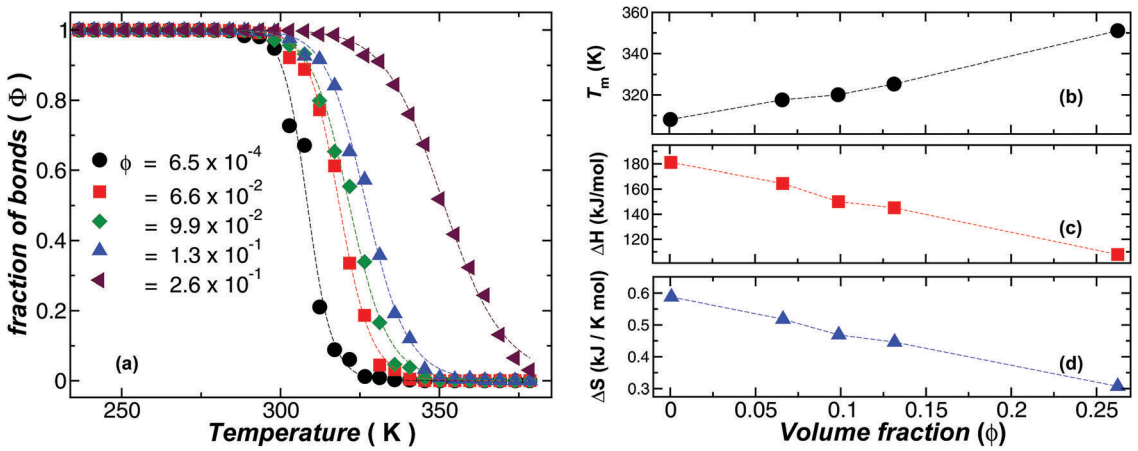

Fig. 14 In panel (a), the fraction of bonds (Φ) as a function of temperature (T) for the disassociation of a dsDNA chain having L = 20 bp interacting withing crowding agents. Here, we vary the volume fraction of crowders ϕ by adding more crowding chains and keeping constant the volume of the simulation box. The symbols represent the data and the lines are fits to eqn (4). Panels (b), (c) and (d) show T_m, ΔH, and ΔS as a function of ϕ. We find that T_m increases with ϕ, but ΔH and ΔS become smaller for smaller ϕ.

V. EEC in simulated duplex DNA melting

The EEC phenomena has often been observed in the melting of dsDNA for chains having different lengths and/or sequences. However, it is not yet clear what factors control the movement along the compensation line. A previous Brownian dynamics study by Forrey and coworkers[52] indicated that EEC changes arose from changes in the rigidities of binding polymers and that two regimes existed, a high and a low rigidity regime where the direction of movement along the EEC line was opposite in each regime. Here, we start from a simple coarse-grained model for DNA where the chains have specific associative base-pair interactions and we investigate whether EEC is still observed. We are now in a position to identify molecular variables that influences the direction of movement along the compensation line in the specific context of DNA melting. In Fig. 15, we show that all our data conform to the EEC phenomenon, as observed by experiments, where we have plotted our data in the same formats considered by experimentalists. Note that explicit consideration of the solvent is not required to reproduce this general trend (hydration is no doubt a contributing factor, but this contribution is absorbed in our coarse-grained model parameters such as k_{bend}). The direction of movement along the EEC line can be inferred from changes in the chain rigidity arising from changes of the inherent rigidity of the chain from altering its molecular structure, solvent conditions, or extrinsic changes of rigidity due to the confinement in the presence of crowding molecules.

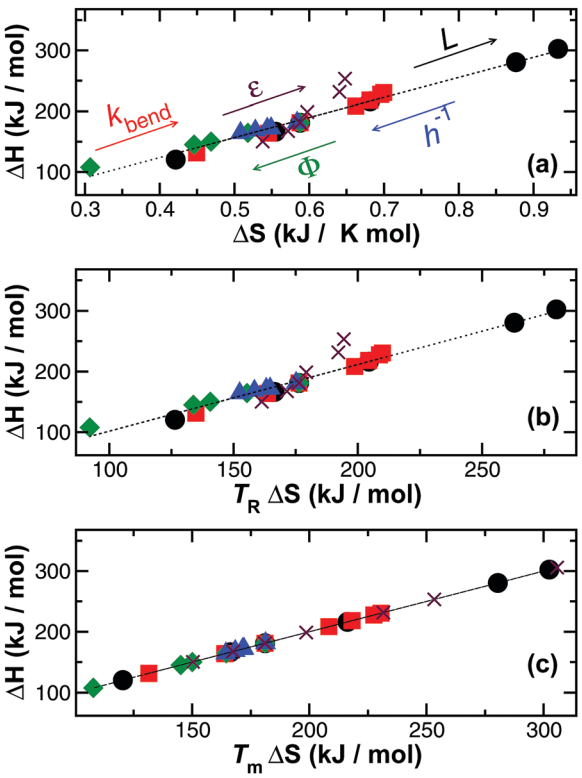

Fig. 15 In panel (a), the change in enthalpy ΔH as a function of the change in entropy ΔS for the simulation results obtained in this manuscript. In panel (b), ΔS has been multiplied by the room temperature T_R = 300 K. In panel (c), ΔS has been multiplied by the dsDNA melting temperature T_m. The fluctuations around the compensation line in panel (b) arise from imperfect EEC due to the variations of T_m, an effect considered in Section V A.

Although we anticipated a general EEC trend with changing rigidity, as in the past work by Forrey and coworkers,[52] we were surprised to find that the direction of movement along the EEC line in Fig. 15 depends on the physical origin of the changes in the chain rigidity. Increasing the intrinsic chain rigidity by altering L, k_{bend}, ε, *etc.*, leads to an increase in both ΔH and ΔS, while the addition of extrinsic constraints on the dsDNA such as increasing confinement $(1/h)$ and ϕ causes ΔH and ΔS to move to the left, corresponding to a decrease in the binding energetic parameters.

These general trends in the movement along the EEC line are quantified by examining the variation of ΔS with the rigidity parameter, κ^0_{ds}. Fig. 16(a) shows the effect of altering intrinsic chain rigidity by varying the chain length L, base pair interaction strength ε and the chain bending parameter k_{bend}. The variation of ΔS is nearly linear with k_{bend}, which is nearly proportional to κ^0_{ss}, so that the rigidification of isolated chains leads to an increase in ΔS and ΔH, other parameters being held fixed. This general trend holds for L and ε also, but the variation of ΔS becomes very sharp as L and ε become large so that κ^0_{ds} approaches its limiting value, $\kappa^\infty_{\mathrm{ds}}$ (see Fig. 6 and 10). This means that the modulation of the energetic parameters for molecular binding is especially strong when the binding molecules are relatively rigid. Fig. 16(b) shows that the introduction of increasing crowding constraints (increasing the concentration of the degree of confinement, $1/h$) leads to a decrease in ΔS and ΔH as the dsDNA rigidifies. The crowding molecules seem to be particularly effective in altering ΔS, although attractive interaction between DNA and the crowding molecules or the boundaries should modulate these effects, as discussed in the next section.

A. Influence of flexibility on T_m: overcoming strict EEC

We have seen that changes in molecular flexibility, as quantified by κ^0_{ds}, serves to modulate the entropy of DNA association ΔS, which, in turn, controls the direction of movement along the EEC curve shown in Fig. 15. The DNA melting temperature T_m, as with the melting of ordinary crystals, is governed by the ratio $T_m = \Delta H/\Delta S$, where ΔH and ΔS are the overall enthalpy and entropy of melting. In the compensation plots discussed above, an average melting temperature $\langle T_m \rangle$ for a series of binding molecules corresponds to the "compensation temperature". However, while the changes of T_m with varying molecular parameters may be relatively small in comparison to changes in ΔH and ΔS, changes in T_m are important practically because they reveal a strategy for modifying the strength of molecular binding at a fixed temperature. This allow us to overcome strict EEC. As discussed in the introduction, this is a primary concern in the development of new drugs having enhanced binding to DNA and other biological macromolecules. We next consider

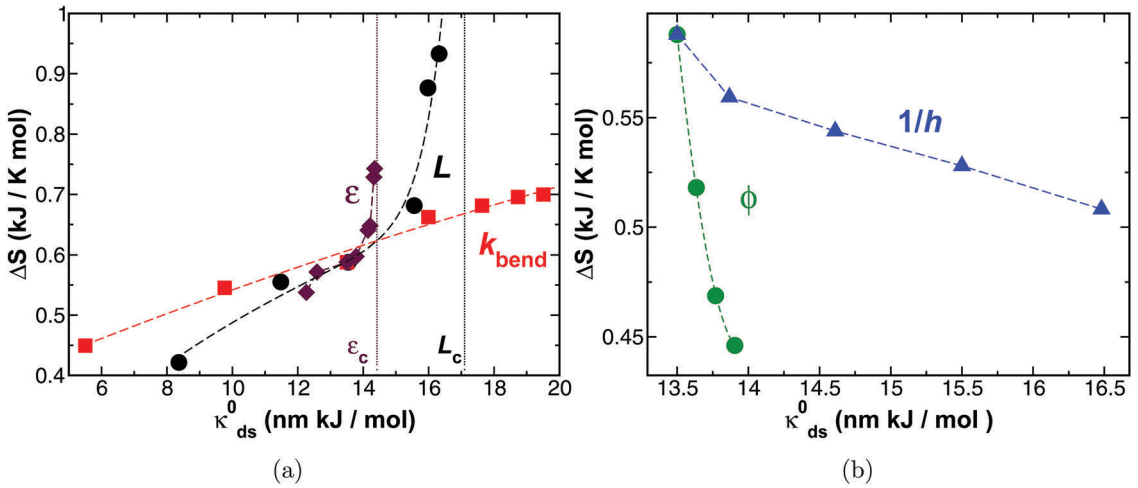

Fig. 16 In (a), change in entropy ΔS as a function of the rigidity parameter κ^0_{ds} modification of the intrinsic chain stiffness (bending parameter k_{bend}, bonding energy ε, or length L). The vertical dashed lines are the plateau values for κ^0_{ds} obtained from eqn (11) (black line) and eqn (12) (maroon line). In (b), change in entropy ΔS as a function of the rigidity changes from extrinsic constraints (confinement h or volume fraction of crowding agents ϕ).

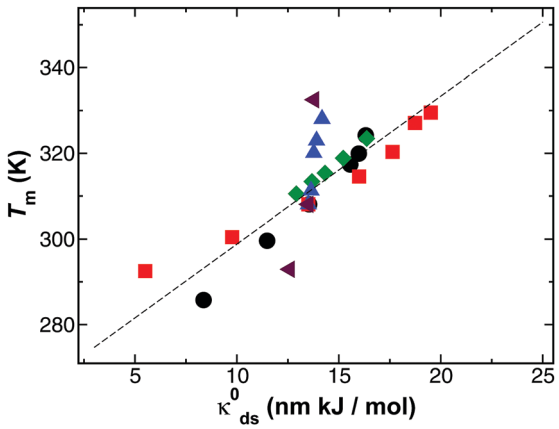

Fig. 17 The melting temperature T_m as a function of the intrinsic rigidity parameter κ^0_{ds}. T_m apparently tends to be higher for more rigid complexes, although attractive interactions between the dsDNA and the confining boundaries or surrounding chains are not considered in this analysis.

how varying κ^0_{ds} influences the stability of duplex DNA through its influence on T_m.

Fig. 17 shows that, in the absence of simultaneously altering other molecular parameters, T_m increases with the change in rigidity κ^0_{ds} for all the systems that we have simulated, regardless of whether this increase arises from a change of the intrinsic rigidity of the dsDNA chain or through external crowding constraints due to confining surfaces or surroundings crowding polymer chains. As mentioned earlier, a counter-example is the addition of salt, where T_m changes due to electrostatic screening are opposite to (and stronger than) changes due to rigidity. The advantage of progressive molecular rigidification in the maturation of antibodies,[6,8,46] mentioned in Section I, is then apparent, *i.e.* intrinsic rigidification of binding molecules tends to cause stronger binding. This tendency of enhanced binding strength with increasing stiffness is also operative locally within binding macromolecules. For example, binding proteins involved in regulating genetic expression bind strongly and selectively to relatively stiff DNA base sequence regions rich in G–C content,[123] and the catalytic binding sites of proteins are relatively stiff regions of the protein.[124]

The changes in the energetic parameters governing molecular binding are evidently strongly coupled to the degrees of freedom of the surrounding crowding molecules. There is further complication that this coupling must depend on the detailed type of interaction between the crowding molecules and the binding species. This is a complex problem deserving a separate investigation, but we briefly discuss this phenomenon to emphasize that confinement and crowding do not generally lead to enhanced binding strength. This effect also offers a practical strategy for "engineering" the strength of molecular binding in practical applications.

Experience with melting and freezing phenomena in other materials reminds us that changes in the boundary interaction can *reverse* the sign of the shifts in T_m.[125,126] Our simulations however are restricted to duplex DNA confined between repulsive walls or surrounded by flexible polymer chains having strong repulsive excluded volume interactions with the duplex DNA. By analogy with other melting processes, we may then expect T_m to exhibit an inverted trend when attractive DNA–surface interaction or DNA–polymer interactions are sufficiently attractive. An effect of this kind would provide a useful means of reducing the magnitude of binding constants, an effect of immense practical value. There is substantial evidence for such an effect. Independent analytic[24] and simulations studies[113,127] have verified this effect for associating proteins subject to crowding by polymer chains having unspecified attractive interactions with the binding species. Simulations have also shown that folded proteins can be destabilized when they are constrained to be near surfaces with attractive interactions with the protein,[128] while proteins tend to become stabilized when confined by repulsive boundaries.[129] Chaperon proteins operate based on this physical effect.[130,131] In contrast, the melting temperature,

T_m, of DNA can be shifted downwards by attractive surface interactions when one of the ends is grafted to a substrate, a matter of some consequence in DNA chips.[132–137] As another practical example, the addition of carboxyl-modified single-walled carbon nanotubes, which interact attractively with ssDNA, destabilizes DNA duplex formation.[122,138] In a materials science context, it has been shown that the addition of extended sheet like nanoparticles, similar in geometry to graphene, can stabilize ZnO quantum dots, and other nanoparticles, against association in polymer matrices.[139]

We are not aware of any experimental studies of DNA duplex stability under confinement by two boundaries having attractive DNA–surface interactions, but shifts in T_m under confinement should be relevant for sequencing methods for DNA involving localizing duplex DNA in pores or other confined geometries employed in rapidly developing technologies related to DNA sequence determination.

It is well known that adding salt such as NaCl to a solution alters the binding energetic parameters between the bases at low ionic strength, but these effects are saturated at salt concentration exceeding about 0.5 M.[140] At such high salt concentrations, charge effects are essentially neutralized, and T_m tends to decrease as l_p decreases, an effect presumably reflecting the trend exhibited in Fig. 17. However, changes in salt and pH can involve a convolution of effects involving changes in both the energetics of base binding and duplex rigidity. Varying ion valence and pH, or the addition of molecules such as dyes and proteins that bind to dsDNA provides additional means of altering the rigidity of DNA.

B. Sharpness $\mathcal{C}$ of DNA melting transition

In addition to the strength of DNA duplex binding, the "sharpness" or "cooperativity"[141] of the melting transition, defined in terms of the temperature range over which the melting occurs, is another basic aspect of DNA duplex formation and melting that is central in applications. For example, the high "selectivity" of the binding of ssDNA grafted onto nanoparticles to complementary strands in solution is a consequence of the narrow T range of the melting transition arising from the high grafting density of ssDNA on the nanoparticles.[142,143] We believe that this is just another example of a crowding interaction by surrounding chains, but we have the added complication of DNA interaction with the nanoparticle modulating T_m, which makes it difficult to predict resulting T_m shifts. Within the two-state model of DNA melting, we can calculate the temperature range of the melting transition by simply considering the rate of change in the order parameter Φ with respect to temperature at the melting temperature. In particular, sharpness or cooperativity $\mathcal{C}$ of the melting transition is defined as,

$$\mathcal{C} = \left.\frac{d\Phi(T)}{dT}\right|_{T=T_m} = \Delta S^2/(4k_B\Delta H) = \Delta S/(4k_B T_m). \quad (13)$$

As mentioned earlier, a counter example is the addition of salt, where T_m changes due to electrostatic screening are opposite to (and stronger than) changes due to rigidity. We then see that in the event T_m is not greatly altered by changes in the system (often a reasonable approximation in practice) so that $\mathcal{C}$ of the DNA melting transition for a fixed enthalpic interaction strength set by the base sequence is controlled by ΔS and $\mathcal{C}$ is related to the intrinsic rigidity of the binding DNA chains. Since the variation of ΔS with κ_{ds} depends on whether the rigidity changes are due to changes in the molecular structure of the DNA molecule or external constraints, $\mathcal{C}$ can either increase or decrease with the rigidity of the duplex DNA, corresponding to a sharper or broader melting transition, respectively.

VI. Conclusions

It is broadly appreciated in the biological community that the alteration of the rigidity upon molecular binding plays a large role in controlling the strength and selectivity of molecular binding, but the quantification of this effect has been difficult. Our goal was to explore a model binding system, duplex DNA, where the energetic parameters governing binding can be controlled by varying molecular parameters (DNA sequence, chain length, salt concentration) that alter the intrinsic rigidity of the duplex DNA and by extrinsic constraints, such as geometrical confinement between slits or by crowing molecules in the environment of the DNA duplex to determine how molecular rigidity, obtained from the persistence length of the duplex DNA and ssDNA, influences the energetic parameters governing duplex stability. Since the persistence length is not universally applicable as a measure of molecular "flexibility" in binding molecules, we also considered other measures of DNA flexibility that should be more transferable to protein binding and other molecular binding processes to make estimates of molecular rigidity more experimentally accessible for studies aimed at "engineering" molecular binding strength for a wide variety of applications.

Quantifying the flexibility of duplex DNA involves physical effects that are not incorporated into continuum polymer models, such as a worm-like chain model. Changes in the rigidity related to the dissociation of the nucleic acid bases have to be considered in order to reliably estimate a rigidity parameter κ^0_{ds} for characterizing how rigidity influences the binding energetic parameters of duplex DNA. The quantification of rigidity in ssDNA proved more difficult than we expected because of the inapplicability of the worm-like chain model to flexible chains.

After establishing our measure of rigidity (κ^0_{ds}), we focused our attention on how varying κ^0_{ds} alters the energetic parameters of duplex formation, ΔH and ΔS. First, we demonstrated that our simulations give rise to an enthalpy–entropy compensation (EEC) relationship similar to that observed in experiments, where this phenomenon is observed without any explicit consideration of water. Changes in κ^0_{ds} were found to be correlated strongly with the direction of movement on the EEC plot. In particular, the direction of motion on the EEC line was found to be controlled by the variation of the entropy of duplex formation ΔS; this quantity increases with κ^0_{ds} when the changes in duplex rigidity derive from intrinsic molecular parameters of the DNA molecular complexes, in which ΔS decreases with κ^0_{ds}, when the

change in rigidity arises from extrinsic constraints such as confining walls or surrounding chains having non-specific repulsive interactions with the duplex DNA. We expect this trend to be general for diverse other binding macromolecules of interest in biology and manufacturing.

We briefly considered two other aspects of the DNA melting transition that have practical significance for understanding and engineering molecular binding: the sharpness or ''cooperativity'' $\mathcal{C}$ of the melting transition and the melting temperature itself. Both of these aspects of molecular binding are likewise modulated by duplex DNA rigidity. In particular, we find that the dsDNA melting temperature T_m increases with rigidity κ^0_{ds} for all cases we consider so that greater rigidity tends to promote stronger molecular binding at a fixed temperature, although the enthalpy–entropy compensation effect often means that the magnitude of this effect is often not very large. The sharpness $\mathcal{C}$ of the DNA melting transition normally tracks the entropy of activation ΔS, which means that the changes in $\mathcal{C}$ can either increase or decrease with chain rigidity, depending on how the changes in rigidity arise (intrinsic molecular parameter on extrinsic constraints acting on the duplex DNA). This phenomenon obviously deserves further study in view of the many applications related to the control of $\mathcal{C}$. We briefly mention some new areas of investigation based on the approach developed in the present paper.

In many binding molecules, only a part of the molecule is involved in the binding to another molecular species. For example, telomere complexes at the end of duplex DNA, clearly influence the stability of the duplex DNA and presumably the primary function of DNA of the expression of its genetic information.[144] Hairpin loops form with RNA and the ends of RNA associate to form a binding complex where the local base pairing is similar to duplex DNA. The presence of these loops modulates the stability of RNA binding complexes.[145] Finally, the binding of ligands to proteins occurs at specific ''binding pockets'' within the protein where the rest of the molecule serves to modulate the binding thermodynamics and dynamics. We can expect the principles described in the present paper to be applicable in these diverse binding processes crucial to living systems.

Changes in the local rigidity within the molecular binding clearly deserve further study in the future. The estimation of rigidity changes in chemically heterogeneous molecules will require other measures of rigidity, such as the Debye–Waller factor (See Appendix B), to determine rigidity changes related to binding strength. Many quantitative studies of this kind already exist, but it would be useful to make these studies move quantitative.

Whitesides and coworkers[146] have made an interesting series of measurements that provide a natural starting point for computational studies emphasizing local rigidity changes in relation to molecular binding. They attached a non-associating flexible chain to a molecule that binds with a fixed ligand where the length of the flexible chain was varied and found clear EEC in the binding energetic parameters as found in DNA hybridization. We expect this effect to again arise from a change in the molecular rigidity (conformational entropy) of the molecule as a whole by attaching the non-binding fragments, creating non-local changes in the dynamics of the molecule.[147] This would seem to provide a model system for understanding allosteric effects in proteins where changes in molecular structure far from the binding site can significantly alter binding thermodynamics.[9] We plan to consider this problem in a future work.

Since the binding process of biological materials requires molecular binding constants to lie within operational ranges for the viability of organisms and for the preservation of biological materials, an understanding of how to manipulate binding constants according to the principles described in the present paper has numerous technological applications associated with the preservation of tissue, proteins, cells, *etc.* Surveys of the thermostability of diverse biological systems (*e.g.* tissues, cells, and proteins) under hyperthermic injury leads to a loss of viability and activity that follows EEC.[148,149] A dynamic version of EEC has recently been studied intensively in the context of preserving proteins and drugs in sugar matrices where EEC is observed and modulated by modifying the rigidity of the glassy sugar matrix with molecular additives such as glycerol.[150–152] Moisture often has a significant influence on the rigidity of biological materials and EEC has been observed in the preservation of foods as moisture content is varied.[153,154] In the future, we plan to study how engineering the rigidity of materials can be used to enhance the preservation of tissue cells, proteins, and other biological materials.

Conflicts of interest

There are no conflicts to declare.

Appendix A: calculation of the persistence length for ssDNA chains

The persistence length (l_p^{ss}) for a ssDNA chain is defined as the average projection of the chain end-to-end distance $\mathbf{R}_e$ on the first bond of chain $\mathbf{l}_1$,[84]

$$l_p^{ss} = \langle \mathbf{R}_e \cdot \mathbf{l}_1 \rangle / \langle l_1 \rangle. \quad \text{(A1)}$$

Fig. 18(a) shows the temperature dependence of l_p^{ss} for chains formed by 20 bases, where we vary the stiffness constant k_{bend} from 0 kJ mol^{-1} to 14 kJ mol^{-1}. We find a linear relation between l_p^{ss} and the reciprocal of T,

$$l_p^{ss}(T) = \delta l_p^{ss} + \frac{\kappa^0_{ss}}{k_B T}. \quad \text{(A2)}$$

Here, κ^0_{ss} and δl_p^{ss} are fitting parameters that do not depend on T, but they both depend on k_{bend}, as is shown in panels (b and c) of Fig. 18, respectively. In Fig. 18(b), the black circles are the data and the red dashed line is a fit of the data to the relationship,

$$\delta l_p^{ss} = \delta l_p^{ss}(k_{bend} = 0)\exp[-(k_{bend}/k_{bend}^{\star})^2], \quad \text{(A3)}$$

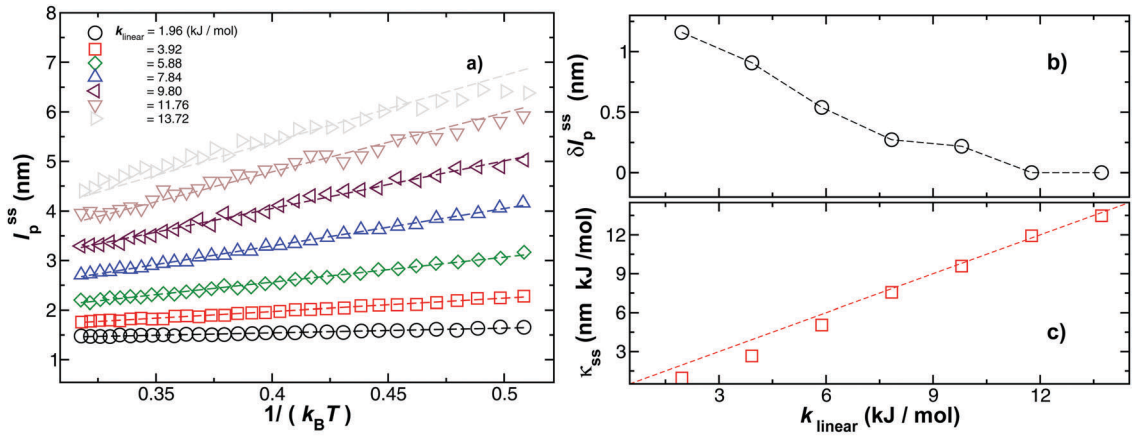

Fig. 18 Panel (a) shows the persistence length for ssDNA having different k_{bend} as a function of the reciprocal temperature. For all these systems, the chain length and bonding energy have been fixed, L = 20 bases and ε = 19.67 kJ mol^{-1}. The symbols are the data and the dashed lines are fits to eqn (A1). In (b and c) we show the fitting parameters δl_p^{ss} and κ_{ss}^0, respectively, obtained from (a) as a function of k_{bend}. Simple relationships for the k_{bend} dependence on δl_p^{ss} and κ_{ss}^0 are provided in the text.

where k_{bend}^* = 6.62 kJ mol^{-1} is the only fitting parameter. Here, $\delta l_p^{ss}(k_{bend} = 0)$ depends in general on both, the maximum bond length R_0 and the bead diameter σ, and for this particular model, it is altered by the inner-chain interaction potential given by eqn (3) in the main text. For the current model, $\delta l_p^{ss}(k_{bend} = 0)$ = 1.22 nm. In Fig. 18(c), the black squares are the data and the red dashed line indicates that κ_{ss}^0 and k_{bend} are essentially equal.

The constant term δl_p^{ss} is not expected from the simple worm-like chain model[87] in which polymers are treated in terms of macroscopic continuum elasticity theory and we did not anticipate this contribution to l_p^{ss}. However, it has recently become appreciated that thermal fluctuations "renormalize" the "bare" value of stiffness parameter κ_{ss}^0 of semi-flexible polymers derived from continuum theory.[87] As discussed by Gutjahr *et al.*,[87] there are contradictory predictions on even the sign of these fluctuation corrections to κ_{ss}^0, depending on the definitions of persistence length and other assumptions, but there is general accord on the *existence* of these fluctuation corrections to l_p. Unfortunately, there seems to be no previous MD simulations of l_p^{ss} that clarify the specific nature of these fluctuations effects. The situation is clearer, however, for the theoretically estimated shift in κ_{ss}^0 associated with the buckling transition of semi-flexible polymers. In particular, Gutjahr *et al.*[87] predicted that the effective κ_{ss}^0 value associated with the chain buckling counterintuitively increases with an increase in amplitude of the thermal fluctuations (*i.e.*, heating). The thermal fluctuation correction to the chain rigidity is positive and proportional to k_BT, an effect similar to the thermoelastic stiffening of rubbery materials upon heating.[155] This fluctuation renormalization of κ_{ss}^0 is qualitatively consistent with eqn (A2) and with earlier arguments for fluctuation renormalization of rigidity by Pinnow and Helfrich[156] in the context of semi-flexible membranes. We note that the presence of a positive and T independent "static" contribution to the persistence length has been noted in previous experimental studies of DNA.[157,158] We did not anticipate the existence of δl_p^{ss} in our analysis of ssDNA rigidity, but after accounting for these fluctuation contributions to chain stiffness, we may determine κ_{ss}^0 as a measure of polymer rigidity. These fluctuation effects have implications for many recent experimental studies that try to infer κ_{ss}^0 and the related Young's modulus from l_p data;[94,106,159] these studies neglect the thermal fluctuation contribution that we discussed here. We suggest that the neglect of this contribution to κ_{ss}^0 might in some cases lead to an appreciable error in estimates of the chain bending modulus. While errors from this assumption should be rather small for rigid fiber structures, such as tubulin[94] and carbon nanotubes,[159] they should be more appreciable for more flexible structures such as ssDNA. Baumann *et al.*[106] have also recently stressed the limitations of continuum modeling of the elastic properties of DNA.

Appendix B: Debye–Waller factor as another measure of molecular rigidity

The Debye–Waller factor $\langle u^2 \rangle$, often referred to in the literature on biomolecular structures as the mean-square displacement (RMSD), has emerged as a general measure of local rigidity,[147,160,161] "softness" or "resilience" in biological macromolecules and many studies have recently performed showing that this quantity can provide information about the relative thermodynamic stability of folded proteins and other practically important biological structures. As noted before, this quantity can be estimated with relatively high precision from neutron, X-ray, and other scattering methods, and in favorable instances when the molecule can be crystallized, $\langle u^2 \rangle$ can be determined for the atoms within the molecule, providing a precise indication of local variations of local molecular

flexibility and variations upon molecular binding or mutation of the molecule. This is a valuable source of information about local molecular flexibility,[10] which can also be determined readily by molecular dynamics simulation. We also mention the "dynamical order parameter" (S^2) obtained by NMR measurements,[162] which conveys similar information to $\langle u^2 \rangle$,[9] and which, in combination with simple models, has been used to estimate the conformational entropy of proteins.[9] The rate of hydrogen–deuterium exchange between the biopolymer and surrounding water molecules is yet another commonly employed measure of local molecular "flexibility".[161] Among these various measures of local flexibility, the estimation of $\langle u^2 \rangle$ values seems to be the most "transferable" measure of flexibility between different types of binding molecules, making this an attractive quantity in relation to quantifying the rigidity of DNA.

To determine $\langle u^2 \rangle$, we first compute the translational mean square displacement of the chain $\langle r^2(\Delta t) \rangle$ giving by,

$$\langle r^2(\Delta t) \rangle \equiv \frac{1}{N} \sum_{i=0}^{N-1} \left\langle |\vec{r}_i(t') - \vec{r}_i(t)|^2 \right\rangle, \quad \text{(B1)}$$

where $\vec{r}_i(t')$ and $\vec{r}_i(t)$ are the positions of bead i that form the chain at times t' and t, respectively, and $\Delta t = t' - t$. Fig. 19(a) shows example calculations of $\langle r^2(\Delta t) \rangle$ for a dsDNA chain formed by 15 bp before and after the dsDNA melts. The different colors represent different values of temperature.

We determine the Debye–Waller Factor $\langle u^2 \rangle$ as the value of $\langle r^2(\Delta t) \rangle$ for which the following condition is fulfilled,

$$\frac{\partial \ln \langle r^2(\Delta t) \rangle}{\partial \ln(\Delta t)} = 0. \quad \text{(B2)}$$

This condition is represented in Fig. 19(a) by a black vertical line. Fig. 19(b) shows $\langle u^2 \rangle$ obtained from Fig. 19(a) as a function of temperature. In the region where $T \ll T_m$, $\langle u^2 \rangle$ is roughly linear with T, from where we extract information about the intrinsic rigidity of the duplex DNA. We compute $\langle u^2 \rangle$ for all the base pairs in a dsDNA in the ordered region $T \ll T_M$.

Fig. 20 shows that these estimates of $\langle u^2 \rangle$ with variable k_{bend} can be well described by a simple harmonic approximation,

$$\langle u^2 \rangle = k_B T / k_{harm}, \quad \text{(B3)}$$

where k_{harm} represents an "effective force constant" that characterizes the "softness" of the molecule. We also plot k_{harm} *versus* k_{bend} in the right panel of Fig. 20 where we find a strong correlation between these two quantities. Evidently, k_{harm} provides an alternative measure of the rigidity of duplex DNA. However, given the redundancy of the information contained in this property with κ_{ds}, we emphasize κ_{ds} in the main text as our basic measure of duplex DNA rigidity. In summary, we find that $\langle u^2 \rangle$ provides a good alternative measure of stiffness of dsDNA which should be useful for studying the binding of molecules having significant chemical heterogeneity, *e.g.*, proteins. We also point out that since the increase of $\langle u^2 \rangle$ provides an estimate of the relative configurational entropy of the molecule, as estimated by $\langle S^2 \rangle$, *etc.*,[162] we see from eqn (B3) that there is a general inverse relation between molecular rigidity and configurational entropy. Correspondingly, we could have equally focused on configurational entropy of the bound molecular complex as a primary factor controlling entropy–enthalpy compensation, but the problem with this approach is that the configurational entropy is rather difficult to calculate and to experimentally estimate.[163–165] The inverse relation between rigidity and configurational entropy has recently been discussed at length in the context of glass-forming liquids.[166]

Disclaimer

This article identifies certain commercial materials, equipment, or instruments to specify experimental procedures. Such identification implies neither recommendation or endorsement by the

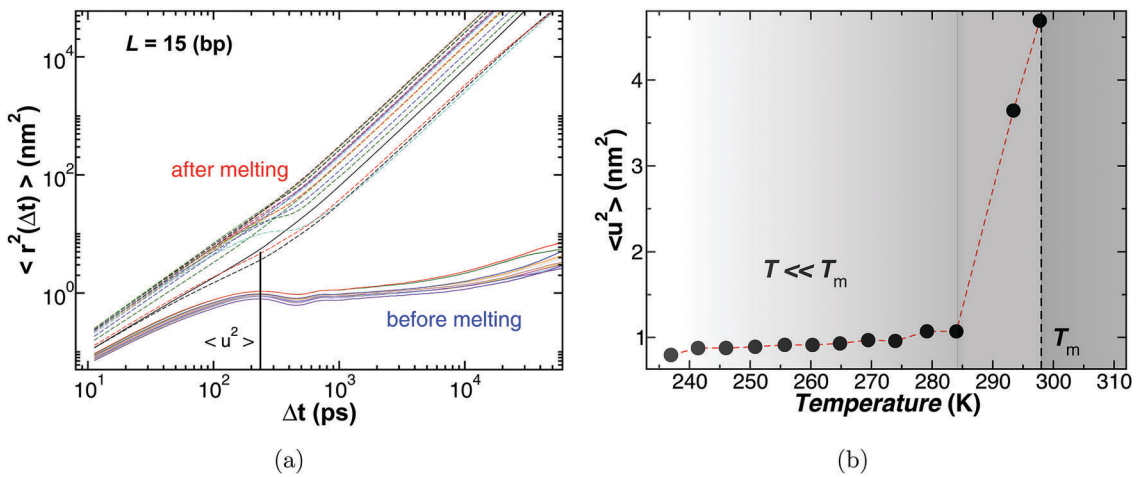

Fig. 19 In the left panel, we show translational mean square displacement for the monomers that form the dsDNA chain as a function of time. Each curve represents a dsDNA at a given value of temperature. The intersection between the vertical solid line and the data defines the Debye–Waller factor $\langle u^2 \rangle$. In the right panel, we show the Debye–Waller factor $\langle u^2 \rangle$ obtained from the left panel as a function of temperature. In the region where $T \ll T_m$, $\langle u^2 \rangle$ is roughly linear with T, from where we extract information about the intrinsic rigidity of the duplex DNA.

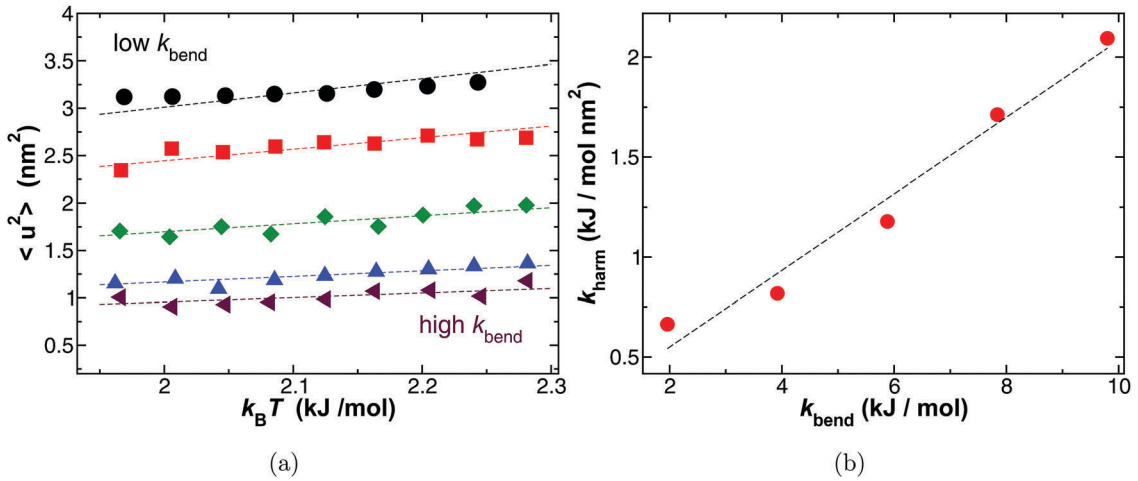

Fig. 20 The left panel shows an example calculation for the average Debye–Waller factor $\langle u^2 \rangle$ as a function of the temperature for dsDNA chains having L = 20 bp and different k_{bend}. In the right panel, the "effective force constant" k_{harm} shows good correlation with k_{bend}, proving k_{harm} to be a good candidate for the characterization of the chain rigidity.

National Institute of Standards and Technology nor that the materials or equipment identified were necessarily the best available for the purpose.

Acknowledgements

This work was supported by NIST awards 70NANB13H202 and 70NANB15H282.

References

1 C. Mattos, G. A. Petsko and M. Karplus, *J. Mol. Biol.*, 1994, **238**, 733.
2 C. Kleanthous, *Protein–protein Recognition*, Oxford University Press, New York, 2000.
3 K. L. Seldeen, C. B. McDonald, B. J. Deegan, V. Bhat and A. Farooq, *Biochemistry*, 2009, **48**, 12213.
4 A. V. Mikecz, *Open Biol. J.*, 2009, **2**, 193.
5 J. Rinnenthal, B. Klinkert, F. Narberhaus and H. Schwalbe, *Nucleic Acids Res.*, 2010, **38**, 3834.
6 M. Mandal, B. Boese, J. E. Barrick, W. C. Winkler and R. R. Breaker, *Cell*, 2003, **113**, 577.
7 A. T. Fenley, H. S. Muddana and M. K. Gilson, *Proc. Natl. Acad. Sci. U. S. A.*, 2012, **109**, 20006.
8 M. C. Thielges, J. Zimmermann, W. Yu, M. Oda and F. E. Romesberg, *Biochemistry*, 2008, **47**, 7237.
9 S.-R. Tzeng and C. G. Kalodimos, *Nature*, 2012, **488**, 236.
10 C. Diehl, O. Engstrm, T. Delaine, M. Hkansson, S. Genheden, K. Modig, H. Leffler, U. Ryde, U. J. Nilsson and M. Akke, *J. Am. Chem. Soc.*, 2010, **132**, 14577.
11 L. Liu, C. Yang and Q.-X. Guo, *Biophys. Chem.*, 2000, **84**, 239.
12 R. R. Swezey and G. N. Somero, *Biochemistry*, 1985, **24**, 852.
13 H. S. Steinert, J. Rinnenthal and H. Schwalbe, *Biophys. J.*, 2012, **102**, 2564.
14 P. Wu, S.-i. Nakano and N. Sugimoto, *Eur. J. Biochem.*, 2002, **269**, 2821.
15 S. Y. Park, A. Lytton-Jean, B. Lee, S. Weigand, G. Schatz and C. Mirkin, *Nature*, 2008, **451**, 553.
16 D. Nykypanchuk, M. Maye, D. V. der Lelie and O. Gang, *Nature*, 2008, **451**, 549.
17 D. Schiffels, T. Liedl and D. K. Fygenson, *ACS Nano*, 2013, **7**, 6700.
18 X. Tu, S. Manohar, A. Jagota and M. Zheng, *Nature*, 2009, **460**, 250.
19 J. D. Chodera and D. L. Mobley, *Annu. Rev. Biophys.*, 2013, **42**, 121.
20 L. Pauling and M. Delbrück, *Science*, 1940, **92**, 77.
21 B. K. Shoichet, *Nature*, 2004, **432**, 862.
22 G. Schneider, *Nat. Rev. Drug Discovery*, 2010, **9**, 273.
23 M.-Y. R. Wang, B. M. Hoffman, S. J. Shire and F. R. N. Gurd, *J. Am. Chem. Soc.*, 1979, **101**, 7394.
24 J. F. Douglas, J. Dudowicz and K. F. Freed, *Phys. Rev. Lett.*, 2009, **103**, 135701.
25 M. Jiao, H.-T. Li, J. Chen, A. P. Minton and Y. Liang, *Biophys. J.*, 2010, **99**, 914.
26 S. Sukenik, L. Sapir and D. Harries, *Curr. Opin. Colloid Interface Sci.*, 2013, **18**, 495.
27 K. F. Freed, *J. Phys. Chem. B*, 2011, **115**, 1689.
28 J. Dudowicz, K. F. Freed and J. F. Douglas, *J. Chem. Phys.*, 2015, **142**, 214906.
29 B. Widom, P. Bhimalapuram and K. Koga, *Phys. Chem. Chem. Phys.*, 2003, **5**, 3085.
30 R. Schmid, A. M. Miah and V. N. Sapunov, *Phys. Chem. Chem. Phys.*, 2000, **2**, 97.
31 J. Dudowicz, J. F. Douglas and K. F. Freed, *J. Chem. Phys.*, 2017, **147**, 064909, DOI: 10.1063/1.4996921.
32 R. Lumry, R. Biltonen and J. F. Brandts, *Biopolymers*, 1966, **4**, 917.
33 D. H. Leung, R. G. Bergman and K. N. Raymond, *J. Am. Chem. Soc.*, 2008, **130**, 2798, pMID: 18257565.

34 V. Kocherbitov and T. Arnebrant, *Langmuir*, 2010, **26**, 3918, pMID: 19904957.
35 A. Pan, T. Biswas, A. K. Rakshit and S. P. Moulik, *J. Phys. Chem. B*, 2015, **119**, 15876.
36 E. B. Starikov and B. Nordén, *J. Phys. Chem. B*, 2007, **111**, 14431.
37 E. B. Starikov, D. Hennig and B. Norden, *Biophys. Rev. Lett.*, 2008, **03**, 343.
38 E. B. Starikov and B. Nordén, *J. Phys. Chem. B*, 2009, **113**, 11375.
39 E. B. Starikov and B. Nordén, *Appl. Phys. Lett.*, 2012, **100**, 193701.
40 The formation of duplex DNA, as well as RNA and protein folding, can be reasonably modeled in terms of the two-state model.[13,14,101].
41 P. Gilli, V. Ferretti, G. Gilli and P. A. Borea, *J. Phys. Chem.*, 1994, **98**, 1515.
42 C. H. Reynolds and M. K. Holloway, *ACS Med. Chem. Lett.*, 2011, **2**, 433.
43 A. Ferrante and J. Gorski, *J. Mol. Biol.*, 2012, **417**, 454.
44 T. S. G. Olsson, J. E. Ladbury, W. R. Pitt and M. A. Williams, *Protein Sci.*, 2011, **20**, 1607.
45 J. Zimmermann, E. L. Oakman, I. F. Thorpe, X. Shi, P. Abbyad, C. L. Brooks, S. G. Boxer and F. E. Romesberg, *Proc. Natl. Acad. Sci. U. S. A.*, 2006, **103**, 13722.
46 J. Kang and A. S. Warren, *Mol. Immunol.*, 2007, **44**, 36233624.
47 R. Adhikary, W. Yu, M. Oda, J. Zimmermann and F. E. Romesberg, *J. Biol. Chem.*, 2012, **287**, 27139.
48 L. Pascale, S. Azoulay, A. D. Giorgio, L. Zenacker, M. Gaysinski, P. Clayette and N. Patino, *Nucleic Acids Res.*, 2013, **41**, 5851.
49 M. De, C.-C. You, S. Srivastava and V. M. Rotello, *J. Am. Chem. Soc.*, 2007, **129**, 10747.
50 L. Liu and Q.-X. Guo, *Chem. Rev.*, 2001, **101**, 673.
51 T. Psurek, C. L. Soles, K. A. Page, M. T. Cicerone and J. F. Douglas, *J. Phys. Chem. B*, 2008, **112**, 15980.
52 C. Forrey, J. F. Douglas and M. K. Gilson, *Soft Matter*, 2012, **8**, 6385.
53 R. Grünberg, M. Nilges and J. Leckner, *Structure*, 2006, **14**, 683.
54 T. J. Kamerzell and C. R. Middaugh, *J. Pharm. Sci.*, 2008, **97**, 3494.
55 F. W. Starr and F. Sciortino, *J. Phys.: Condens. Matter*, 2006, **18**, L347.
56 F. Vargas-Lara and F. W. Starr, *Soft Matter*, 2011, **7**, 2085.
57 O. Padovan-Merhar, F. Vargas-Lara and F. W. Starr, *J. Chem. Phys.*, 2011, **134**, 244701.
58 C. Chi, F. Vargas-Lara, A. V. Tkachenko, F. W. Starr and O. Gang, *ACS Nano*, 2012, **6**, 6793.
59 T. E. Ouldridge, I. G. Johnston, A. A. Louis and J. P. K. Doye, *J. Chem. Phys.*, 2009, **130**, 065101.
60 A. F. Ghobadi and A. Jayaraman, *Soft Matter*, 2016, **12**, 2276.
61 K. Kremer and G. S. Grest, *J. Chem. Phys.*, 1990, **92**, 5057.
62 K. Venta, G. Shemer, M. Puster, J. A. Rodríguez-Manzo, A. Balan, J. K. Rosenstein, K. Shepard and M. Drndi, *ACS Nano*, 2013, **7**, 4629, pMID: 23621759.
63 K. J. Breslauer, R. Frank, H. Blöcker and L. A. Marky, *Proc. Natl. Acad. Sci. U. S. A.*, 1986, **83**, 3746.
64 M. Peyrard, *Acta Phys. Pol., B*, 1994, **25**, 955.
65 T. Dauxois, M. Peyrard and A. R. Bishop, *Phys. Rev. E: Stat. Phys., Plasmas, Fluids, Relat. Interdiscip. Top.*, 1993, **47**, 684.
66 T. Dauxois, M. Peyrard and A. R. Bishop, *Phys. Rev. E: Stat. Phys., Plasmas, Fluids, Relat. Interdiscip. Top.*, 1993, **47**, R44.
67 R. M. Wartell and A. S. Benight, *Phys. Rep.*, 1985, **126**, 67.
68 D. Poland and H. A. Scheraga, *J. Chem. Phys.*, 1966, **45**, 1456.
69 D. Poland and H. A. Scheraga, *J. Chem. Phys.*, 1966, **45**, 1464.
70 C. Richard and A. J. Guttmann, *J. Stat. Phys.*, 2004, **115**, 925.
71 L. A. Marky and K. J. Breslauer, *Biopolymers*, 1987, **26**, 1601.
72 F. H. Stillinger and T. A. Weber, *J. Chem. Phys.*, 1984, **81**, 5095.
73 H. Zhang, M. Khalkhali, Q. Liu and J. F. Douglas, *J. Chem. Phys.*, 2013, **138**, 12A538.
74 N. Theodorakopoulos, *Phys. Rev. E: Stat., Nonlinear, Soft Matter Phys.*, 2008, **77**, 031919.
75 Y. Kafri, D. Mukamel and L. Peliti, *Phys. Rev. Lett.*, 2000, **85**, 4988.
76 Y. Zeng, A. Montrichok and G. Zocchi, *J. Mol. Biol.*, 2004, **339**, 67.
77 W. J. Becktel and J. A. Schellman, *Biopolymers*, 1987, **26**, 1859.
78 F. Vargas-Lara, S. M. Stavis, E. A. Strychalski, B. J. Nablo, J. Geist, F. W. Starr and J. F. Douglas, *Soft Matter*, 2015, **11**, 8273.
79 S. Nosé, *J. Chem. Phys.*, 1984, **81**, 511.
80 W. G. Hoover, *Phys. Rev. A: At., Mol., Opt. Phys.*, 1985, **31**, 1695.
81 S. Plimpton, *J. Comput. Phys.*, 1995, **117**, 1.
82 M. Tuckerman, B. J. Berne and G. J. Martyna, *J. Chem. Phys.*, 1992, **97**, 1990.
83 D. Frenkel and B. Smit, *Understanding Molecular Simulation, Second Edition: From Algorithms to Applications*, Computational Science Series, Academic Press, London, 2001, vol. 1.
84 P. Cifra, *Polymer*, 2004, **45**, 5995.
85 M. Doi and S. F. Edwards, *The Theory of Polymer Dynamics*, Clarendon Press, New York, 1999.
86 M. L. Mansfield, A. Tsortos and J. F. Douglas, *J. Chem. Phys.*, 2015, **143**, 124903, DOI: 10.1063/1.4930918.
87 P. Gutjahr, R. Lipowsky and J. Kierfeld, *EPL*, 2006, **76**, 994.
88 S. Geggier, A. Kotlyar and A. Vologodskii, *Nucleic Acids Res.*, 2011, **39**, 1419.
89 S. Geggier and A. Vologodskii, *Proc. Natl. Acad. Sci. U. S. A.*, 2010, **107**, 15421.
90 K. S. Nagapriya, A. K. Raychaudhuri and D. Chatterji, *Phys. Rev. Lett.*, 2006, **96**, 038102.
91 Note that for DNA chains, l_p^{ss} is $\approx$20 times smaller than l_p.
92 A. Kis, S. Kasas, B. Babić, A. J. Kulik, W. Benot, G. A. D. Briggs, C. Schönenberger, S. Catsicas and L. Forró, *Phys. Rev. Lett.*, 2002, **89**, 248101.
93 J. Danielsson, A. Andersson, J. Jarvet and A. Gräslund, *Magn. Reson. Chem.*, 2006, **44**, S114.

94 F. Gittes, B. Mickey, J. Nettleton and J. Howard, *J. Cell Biol.*, 1993, **120**, 923.
95 J. Huang and L. Gibson, *Mater. Sci. Eng., A*, 1993, **163**, 51.
96 T. P. Knowles, A. W. Fitzpatrick, S. Meehan, H. R. Mott, M. Vendruscolo, C. M. Dobson and M. E. Welland, *Science*, 2007, **318**, 1900.
97 J. Adamcik, J.-M. Jung, J. Flakowski, P. De Los Rios, G. Dietler and R. Mezzenga, *Nat. Nanotechnol.*, 2010, **5**, 423.
98 D. C. Lin, J. F. Douglas and F. Horkay, *Soft Matter*, 2010, **6**, 3548.
99 S. Nakanishi, H. Yoshikawa, S. Shoji, Z. Sekkat and S. Kawata, *J. Phys. Chem. B*, 2008, **112**, 3586.
100 E. Guarnera and I. N. Berezovsky, *Curr. Opin. Struct. Biol.*, 2016, **37**, 1.
101 F. Manyanga, M. T. Horne, G. P. Brewood, D. J. Fish, R. Dickman and A. S. Benight, *J. Phys. Chem. B*, 2009, **113**, 2556.
102 K. F. Freed, *Renormalization Group Theory of Macromolecules*, Wiley, 1987.
103 Y. Seol, J. Li, P. C. Nelson, T. T. Perkins and M. D. Betterton, *Biophys. J.*, 2007, **93**, 4360.
104 Y.-Y. Wu, L. Bao, X. Zhang and Z.-J. Tan, *J. Chem. Phys.*, 2015, **142**, 125103, DOI: 10.1063/1.4915539.
105 F. Pampaloni, G. Lattanzi, A. Jonáš, T. S. E. Frey and E.-L. Florin, *Proc. Natl. Acad. Sci. U. S. A.*, 2006, **103**, 10248.
106 C. G. Baumann, S. B. Smith, V. A. Bloomfield and C. Bustamante, *Proc. Natl. Acad. Sci. U. S. A.*, 1997, **94**, 6185.
107 M. Ikeda-Saito, T. Yonetani, E. Chiancone, F. Ascoli, D. Verzili and E. Antonini, *J. Mol. Biol.*, 1983, **170**, 1009.
108 R. Zwanzig and R. D. Mountain, *J. Chem. Phys.*, 1965, **43**, 4464.
109 V. Ortiz and J. J. de Pablo, *Phys. Rev. Lett.*, 2011, **106**, 238107.
110 G. S. Freeman, D. M. Hinckley, J. P. Lequieu, J. K. Whitmer and J. J. de Pablo, *J. Chem. Phys.*, 2014, **141**, 165103, DOI: 10.1063/1.4897649.
111 J. J. Kasianowicz, E. Brandin, D. Branton and D. W. Deamer, *Proc. Natl. Acad. Sci. U. S. A.*, 1996, **93**, 13770.
112 A. P. Minton, *J. Mol. Biol.*, 1977, **110**, 89.
113 Y. C. Kim and J. Mittal, *Phys. Rev. Lett.*, 2013, **110**, 208102.
114 P. Cuneo, E. Magri, A. Verzola and E. Grazi, *Biochem. J.*, 1992, **281**, 507.
115 K. Richter, M. Nessling and P. Lichter, *J. Cell Sci.*, 2007, **120**, 1673.
116 R. Hancock, *J. Struct. Biol.*, 2004, **146**, 281.
117 D. Miyoshi and N. Sugimoto, *Biochimie*, 2008, **90**, 1040.
118 S. B. Zimmerman and L. D. Murphy, *FEBS Lett.*, 1996, **390**, 245.
119 A. P. Minton, *Biopolymers*, 1981, **20**, 2093.
120 A. P. Minton, *Biophys. J.*, 2000, **78**, 101.
121 A. P. Minton, *J. Biol. Chem.*, 2001, **276**, 10577.
122 X. Li, Y. Peng, J. Ren and X. Qu, *Proc. Natl. Acad. Sci. U. S. A.*, 2006, **103**, 19658.
123 M. E. Hogan and R. H. Austin, *Nature*, 1987, **329**, 263.
124 S. Sacquin-Mora and R. Lavery, *Biophys. J.*, 2006, **90**, 2706.
125 C. Alba-Simionesco, B. Coasne, G. Dosseh, G. Dudziak, K. E. Gubbins, R. Radhakrishnan and M. Sliwinska-Bartkowiak, *J. Phys.: Condens. Matter*, 2006, **18**, R15.
126 P. Z. Hanakata, B. A. P. Betancourt, J. F. Douglas and F. W. Starr, *J. Chem. Phys.*, 2015, **142**, 234907.
127 J. Rosen, Y. C. Kim and J. Mittal, *J. Phys. Chem. B*, 2011, **115**, 2683.
128 I. Knotts, A. Thomas, N. Rathore and J. J. de Pablo, *Biophys. J.*, 2008, **94**, 4473.
129 H.-X. Zhou and K. A. Dill, *Biochemistry*, 2001, **40**, 11289.
130 M. S. Cheung, D. Klimov and D. Thirumalai, *Proc. Natl. Acad. Sci. U. S. A.*, 2005, **102**, 4753.
131 A. Brinker, G. Pfeifer, M. J. Kerner, D. J. Naylor, F. Hartl and M. Hayer-Hartl, *Cell*, 2001, **107**, 223.
132 A. B. Steel, T. M. Herne and M. J. Tarlov, *Anal. Chem.*, 1998, **70**, 4670.
133 T. A. Taton, C. A. Mirkin and R. L. Letsinger, *Science*, 2000, **289**, 1757.
134 J. H. Watterson, P. A. E. Piunno, C. C. Wust and U. J. Krull, *Langmuir*, 2000, **16**, 4984.
135 A. W. Peterson, R. J. Heaton and R. M. Georgiadis, *Nucleic Acids Res.*, 2001, **29**, 5163.
136 J. B. Fiche, A. Buhot, R. Calemczuk and T. Livache, *Biophys. J.*, 2007, **92**, 935.
137 P. Gong and R. Levicky, *Proc. Natl. Acad. Sci. U. S. A.*, 2008, **105**, 5301.
138 X. Li, Y. Peng and X. Qu, *Nucleic Acids Res.*, 2006, **34**, 3670.
139 D. Sun, W. N. Everett, M. Wong, H.-J. Sue and N. Miyatake, *Macromolecules*, 2009, **42**, 1665.
140 S. Tomac, M. Sarkar, T. Ratilainen, P. Wittung, P. E. Nielsen, B. Nordén and A. Gräslund, *J. Am. Chem. Soc.*, 1996, **118**, 5544.
141 L. Qun-li, R. Chun-lai, S. Xiao-hang and M. Yu-qiang, *Sci. Rep.*, 2015, **5**, 9217 EP.
142 R. Jin, G. Wu, Z. Li, C. A. Mirkin and G. C. Schatz, *J. Am. Chem. Soc.*, 2003, **125**, 1643.
143 J. M. Gibbs-Davis, G. C. Schatz and S. T. Nguyen, *J. Am. Chem. Soc.*, 2007, **129**, 15535.
144 G. G. Sharma, A. Gupta, H. Wang, H. Scherthan, S. Dhar, V. Gandhi, G. Iliakis, J. W. Shay, C. S. H. Young and T. K. Pandita, *Oncogene*, 2003, **22**, 131.
145 N. L. Goddard, G. Bonnet, O. Krichevsky and A. Libchaber, *Phys. Rev. Lett.*, 2000, **85**, 2400.
146 V. M. Krishnamurthy, B. R. Bohall, V. Semetey and G. M. Whitesides, *J. Am. Chem. Soc.*, 2006, **128**, 5802.
147 Y. Miao, L. Hong, Z. Yi and J. C. Smith, *Eur. Phys. J. E: Soft Matter Biol. Phys.*, 2013, **36**, 1.
148 B. Rosenberg, G. Kemeny, R. C. Switzer and T. C. Hamilton, *Nature*, 1971, **232**, 471.
149 X. He, *Open Biomed. Eng. J.*, 2011, **5**, 47.
150 A. Anopchenko, T. Psurek, D. VanderHart, J. F. Douglas and J. Obrzut, *Phys. Rev. E: Stat., Nonlinear, Soft Matter Phys.*, 2006, **74**, 031501.
151 R. A. Riggleman, J. F. Douglas and J. J. de Pablo, *Soft Matter*, 2010, **6**, 292.
152 M. T. Cicerone and J. F. Douglas, *Soft Matter*, 2012, **8**, 2983.

153 J. Buitink, M. M. Claessens, M. A. Hemminga and F. A. Hoekstra, *Plant Physiol.*, 1998, **118**, 531.
154 W. Q. Sun, *Plant Physiol.*, 2000, **124**, 1203.
155 M. Gordon, *Br. Polym. J.*, 1976, **8**, 39.
156 H. Pinnow and W. Helfrich, *Eur. Phys. J. E: Soft Matter Biol. Phys.*, 2000, **3**, 149.
157 J. A. Schellman and S. C. Harvey, *Biophys. Chem.*, 1995, **55**, 95.
158 J. Bednar, P. Furrer, V. Katritch, A. Stasiak, J. Dubochet and A. Stasiak, *J. Mol. Biol.*, 1995, **254**, 579.
159 N. Fakhri, D. A. Tsyboulski, L. Cognet, R. B. Weisman and M. Pasquali, *Proc. Natl. Acad. Sci. U. S. A.*, 2009, **106**, 14219.
160 G. Zaccai, *Science*, 2000, **288**, 1604.
161 K. E. Tang and K. A. Dill, *J. Biomol. Struct. Dyn.*, 1998, **16**, 397.
162 M. J. Stone, *Acc. Chem. Res.*, 2001, **34**, 379.
163 S.-H. Chong and S. Ham, *J. Phys. Chem. B*, 2015, **119**, 12623.
164 R. Grunberg, M. Nilges and J. Leckner, *Structure*, 2006, **14**, 683.
165 G. P. Brady and K. A. Sharp, *Curr. Opin. Struct. Biol.*, 1997, **7**, 215.
166 B. A. P. Betancourt, P. Z. Hanakata, F. W. Starr and J. F. Douglas, *Proc. Natl. Acad. Sci. U. S. A.*, 2015, **112**, 2966.